RESULTS AND DISCUSSION

In early work, the simulation runs used a time step of 1.00 fs, and it was found that the system was not going to balance condition. The total energies of bulk water and water confined in nanotubes rose up at the long simulation time (see in Figure 6-left). Although the total energy was not equilibrated, the temperature was well averaged at 298 K. The increase of total energy suggests that the systems were not stable. Therefore, a small time step of 0.25 fs was used and found to be good for the simulation in the canonical *NVT* ensemble with Nosé-Hoover thermostat. Equilibration ensemble was confirmed by the constant of total energy diagram (Figure 6, right hand side). Total energy of bulk water fluctuated within 1.0 kcal mol^{-1} (Figure 6 (a), right), water 77 molecules in (9,9)-SWBNNT fluctuated within 0.08 kcal mol^{-1} (Figure 6 (b), right), water 102 in (10,10)-SWBNNT fluctuated within 0.2 kcal mol^{-1} (Figure 6 (c), right) and other systems see at the second column in Table 3.

Additionally, the total angular momentum was also checked. The total angular momentum of *x*, *y* and *z* components of bulk water (1,000 molecules) were steady at zero (see Figure 7). The total angular momentum of water confined in nanotubes, the smallest tube (water 77 molecules in (9,9)-armchair nanotubes as shows in Figure 8), and the angular momentum *x*, *y* and *z* components were diverting from zero, as it is known that when using periodic boundary conditions, the angular momentum is not conserved.

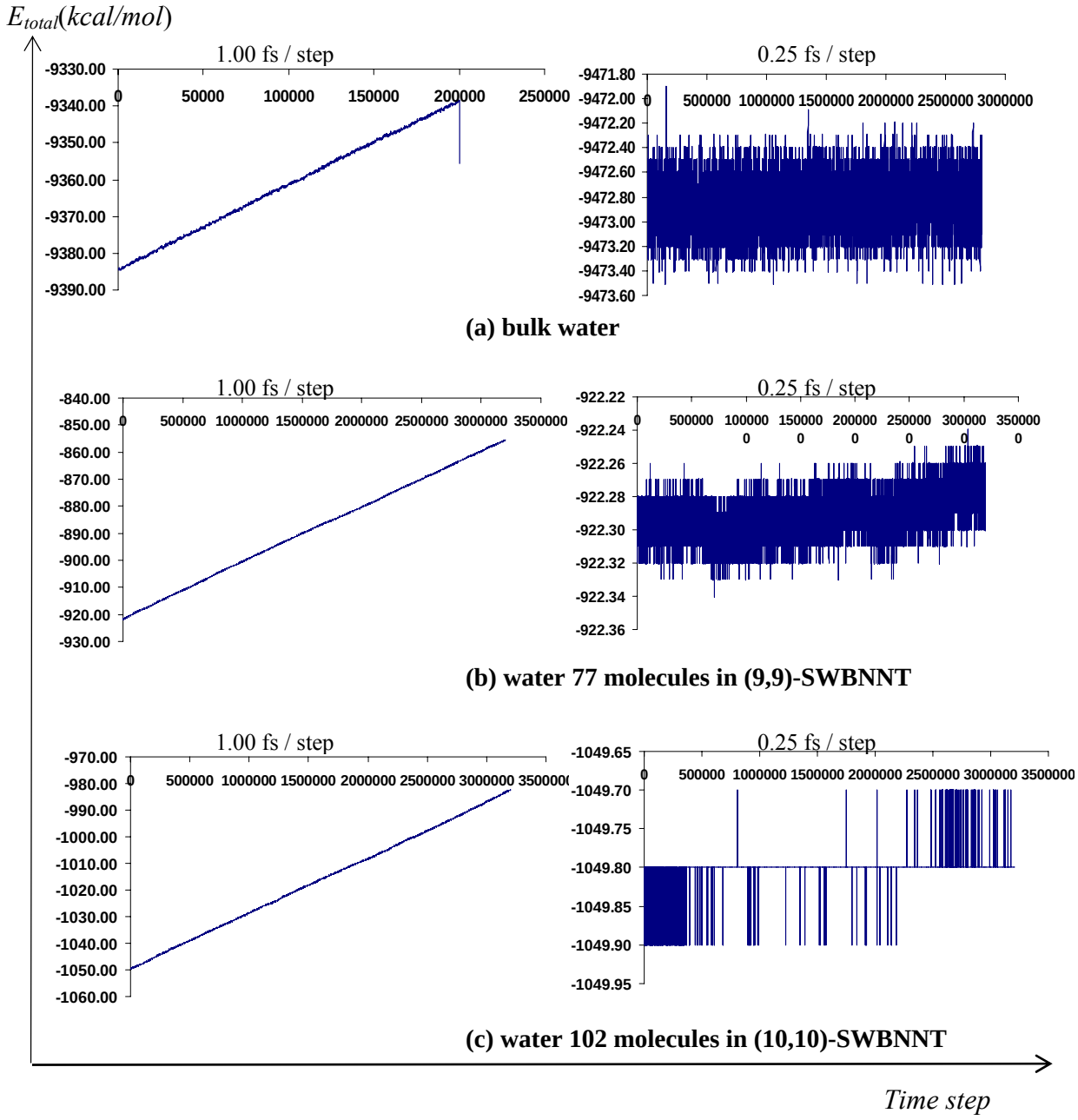

Figure 6 Total energy (kcal mol^{-1}) diagrams show the equilibration of the *NVT* ensemble with Nosé-Hoover thermostat at value of 1.00 fs per a time step (left) and 0.25 fs per a time step (right): total energy of bulk water **(a)**, water 77 molecules in (9,9)-SWBNNT **(b)** and water 102 molecules in (10,10)-SWBNNT **(c).**

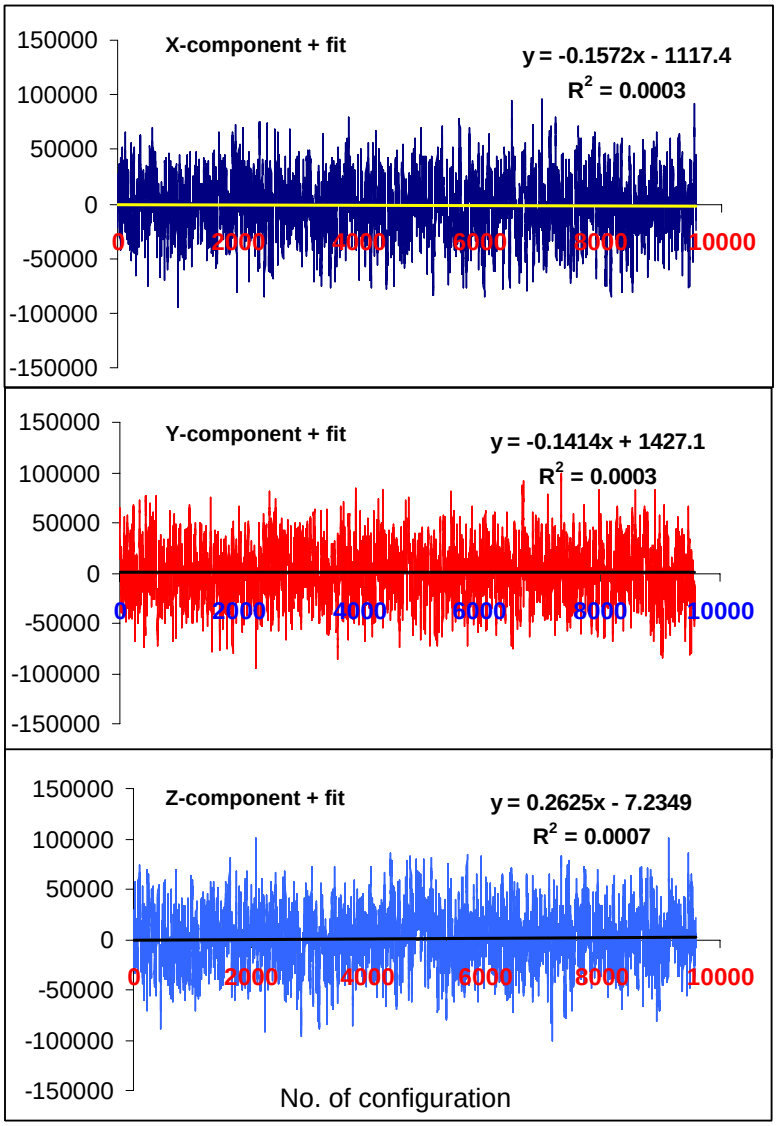

Figure 7 Angular momentum diagram of systems show equilibration state of the *NVT* ensemble with Nosé-Hoover thermostat at value of 0.25 fs per a time step of bulk water (water 1,000 molecules).

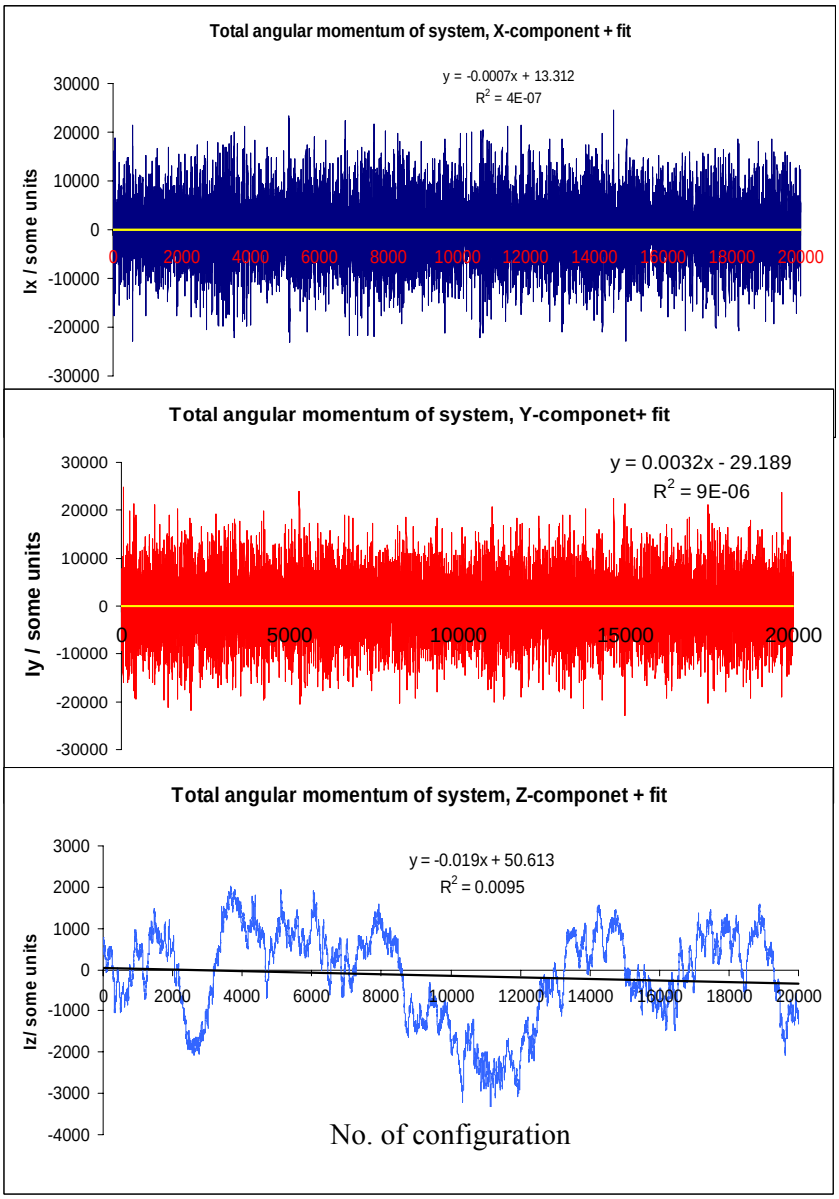

Figure 8 Angular momentum diagrams show equilibration state of the *NVT* ensemble with Nosé-Hoover thermostat at value of 0.25 fs per a time step of water 77 molecules (9,9)-SWBNNTs.

Table 3 Average of total energy (kcal mol^{-1}) and angular momentum (rad s^{-1}) of equilibration systems.

Model	**Average of total energy (kcal mol^{-1})**			**Average of angular momentum of system: Ix, Iy, Iz component**
Bulk water				3×10^{-4}, 3×10^{-4}, 7×10^{-4}
ε_{co} = 0.11433 kcal/mol				
(9,9) - SWCNTa	-885.480	±	0.012	3×10^{-6}, 2×10^{-7}, 8×10^{-2}
(10,10) - SWCNTa	-1041.802	±	0.015	9×10^{-6}, 1×10^{-5}, 3×10^{-4}
(12,12) - SWCNTa	-1591.707	±	0.029	1×10^{-5}, 6×10^{-6}, 3×10^{-2}
(14,14) - SWCNTa	-2302.486	±	0.043	1×10^{-5}, 3×10^{-5}, 3×10^{-3}
(16,16) - SWCNTa	-3156.582	±	0.060	7×10^{-6}, 1×10^{-5}, 1×10^{-3}
(20,20) - SWCNTa	-5373.613	±	0.094	2×10^{-4}, 2×10^{-4}, 4×10^{-4}
ε_{co} = 0.12300 kcal/mol				
(9,9) - SWCNTb	-904.770	±	0.010	6×10^{-8}, 1×10^{-5}, 2×10^{-2}
(10,10) - SWCNTb	-1068.551	±	0.050	2×10^{-5}, 2×10^{-6}, 1×10^{-2}
(12,12) - SWCNTb	-1621.994	±	0.026	2×10^{-7}, 4×10^{-6}, 7×10^{-3}
(14,14) - SWCNTb	-2360.827	±	0.048	9×10^{-5}, 5×10^{-6}, 6×10^{-3}
(16,16) - SWCNTb	-3217.884	±	0.057	3×10^{-6}, 8×10^{-5}, 1×10^{-3}
(20,20) - SWCNTb	-5376.137	±	0.092	3×10^{-4}, 4×10^{-4}, 4×10^{-3}
(9,9) - SWBNNT	-922.298	±	0.010	4×10^{-7}, 9×10^{-6}, 9×10^{-3}
(10,10) - SWBNNT	-1049.805	±	0.021	4×10^{-5}, 1×10^{-6}, 3×10^{-3}
(12,12) - SWBNNT	-1653.444	±	0.050	4×10^{-4}, 2×10^{-5}, 2×10^{-2}
(14,14) - SWBNNT	2431.186	±	0.046	7×10^{-5}, 2×10^{-6}, 2×10^{-2}
(16,16) - SWBNNT	-3287.572	±	0.059	1×10^{-5}, 8×10^{-6}, 1×10^{-3}
(20,20) - SWBNNT	-5373.618	±	0.094	1×10^{-4}, 3×10^{-4}, 7×10^{-4}

Structure comparison of bulk water molecules and water molecules enclosed in different sizes of nanotubes

The radial distribution function (RDF) of water was extracted from the simulation after the system was in equilibrium, and was interpreted to understand the molecular distribution and structure properties of water systems at the deeply molecular level. The results of the radial distribution profiles of bulk water were closed to the results of the neutron diffraction experiment (Soper, 2000). Figure 9 shows the average maximum distances following the 1^{st}, 2^{nd}, 3^{rd} hydration shells: OO distribution of 2.75, 4.55 and 6.79 Å, OH of 1.0, 1.77 and 3.25 Å, and HH of 1.63, 2.40 and 3.99 Å, respectively. The experimental data from neutron diffraction (Kuhs *et al.*, 1984) at 10 K 2.4 GPa reported that the R_{OO} distances were 2.879 and 2.742 Å for H-bonded and non- H-bonded, respectively.

The comparative RDF of bulk water and water confined in nanotubes are shown in Figure 10. The first maximum of all radial distribution functions occurs as a sharp peak at 2.75 - 2.76 Å. The details of the first maximum, first minimum and the average of coordination number n (r) of confined water are presented in the Table 4.

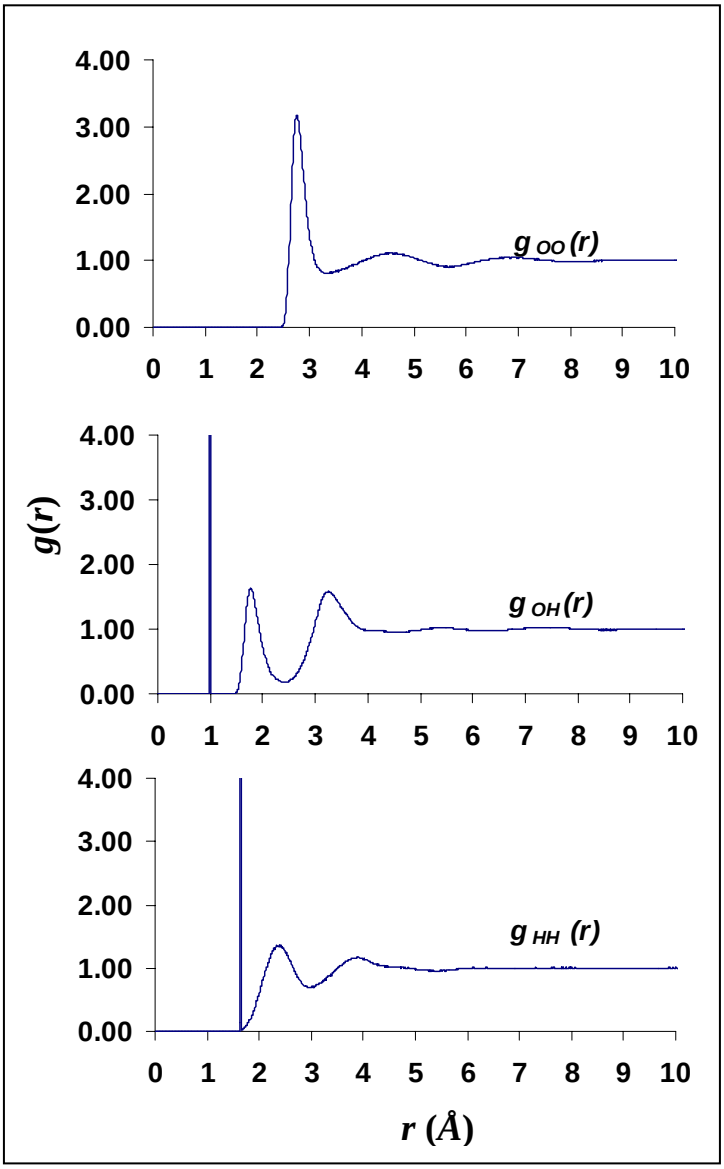

Figure 9 The spherical radial distribution function (RDF) of bulk SPC/E water (1,000 molecules); the partial structure factors of $g_{OO}(r)$, $g_{OH}(r)$ and $g_{HH}(r)$ at the average temperature of 298 K and the water density of 1.00 g cm^{-3}.

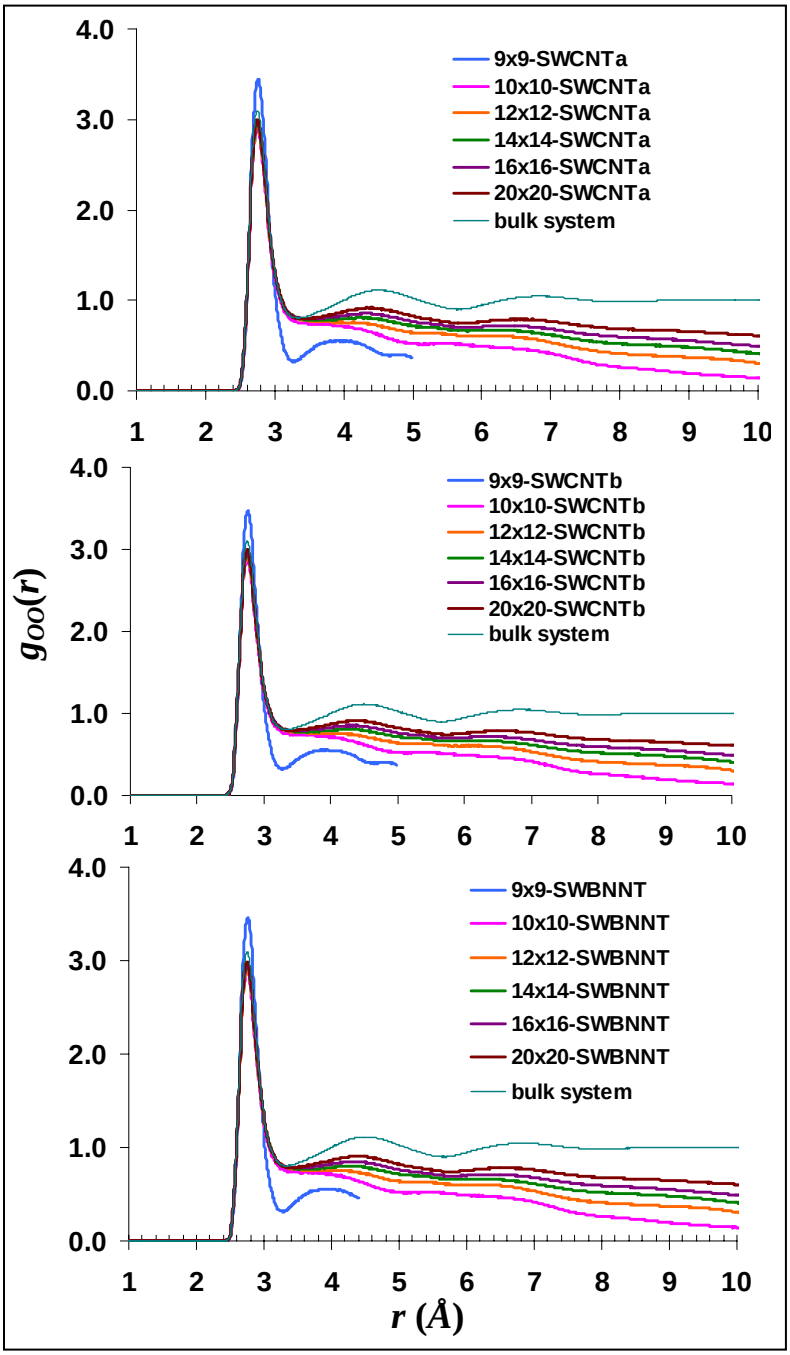

Figure 10 The spherical radial distribution function (RDF) $g_{OO}(r)$ of water confined in SWCNTa of $\varepsilon_{c\text{-}o}$ = 0.1143 kcal mol^{-1} **(a)**, SWCNTb $\varepsilon_{c\text{-}o}$ = 0.1230 kcal mol^{-1} **(b)** and SWBNNT **(c)**; (9,9)-nanotubes: blue, (10,10)-nanotubes: pink, (12,12)-nanotubes: orange, (14,14)-nanotubes: green, (16,16)-nanotubes: violet, (20,20)-nanotubes: brown and bulk system: soft green at the average temperature of 298 K and the water density of 1.00 g cm^{-3}.

Table 4 The results of first maximum and first minimum positions of spherical radial distribution profile $g_{OO}(r)$ of water confined in nanotubes and the average coordination numbers $n(r)$.

Model	**1st Maximum** $g_{OO}(r)$ **(Å)**	**1st Minimum** $g_{OO}(r)$ **(Å)**	**1st Minimum** ***n*(*r*)**
Bulk water	2.75	3.33	4.50
$\varepsilon_{co} = 0.11433$ kcal mol^{-1}			
(9,9) - SWCNTa	2.75	3.27	4.00
(10,10) - SWCNTa	2.75	3.49	4.84
(12,12) - SWCNTa	2.75	3.42	4.71
(14,14) - SWCNTa	2.75	3.46	4.86
(16,16) - SWCNTa	2.75	3.42	4.73
(20,20) - SWCNTa	2.75	3.42	4.70
$\varepsilon_{co} = 0.12300$ kcal mol^{-1}			
(9,9) - SWCNTb	2.76	3.29	4.00
(10,10) - SWCNTb	2.75	3.48	4.79
(12,12) - SWCNTb	2.75	3.49	4.93
(14,14) - SWCNTb	2.75	3.46	4.85
(16,16) - SWCNTb	2.75	3.42	4.72
(20,20) - SWCNTb	2.75	3.42	4.65
(9,9) - SWBNNT	2.76	3.29	3.99
(10,10) - SWBNNT	2.75	3.48	4.79
(12,12) - SWBNNT	2.75	3.48	4.88
(14,14) - SWBNNT	2.75	3.46	4.83
(16,16) - SWBNNT	2.75	3.46	4.82
(20,20) - SWBNNT	2.75	3.44	4.79

In principle, liquid water is classified as a tetrahedral liquid, its coordination number defined as the area under the first peak of the oxygen-oxygen radial distribution function, $g_{OO}(r)$. Based on a geometric definition of averaging over all OO pairs closer than the first minimum in $g_{OO}(r)$, an $n(r)$ above four and below five suggests the presence of liquid water and the four directional hydrogen bonds of ice-like tetrahedral structure (Head-Gordon and Johnson, 2006). According the principle, it was found that the coordination number $n(r)$ of water confined in nanotubes which different attractive interactions of SWCNTa, SWCNTb and SWBNNT are not homogeneous. It is modified by confinement in the nanometer scale regions inside nanotubes. The water confined in smallest (9,9)-SWCNTa, (9,9)-SWCNTb and (9,9)-SWBNNT had an average $n(r)$ at four, and which indicated the ice-like property. While, water in the larger pore diameters (10,10), (12,12), (14,14) (effective diameters of 10.22, 12.92 and 15.62 Å respectively), $n(r)$ is increased. The $n(r)$ is slightly decreased on the effective diameters of 15.62, 18.34 and 23.74 Å: (14,14), (16, 16) and (20,20) respectively. All $n(r)$ of water in the wider pore sizes suggested the liquid-like properties.

The coordination number $n(r)$ and distribution percentage of coordination number were reported because there may be several distribution structures. In case of bulk water, there are coordination numbers of about 4 and 5 as shown in Figure 11. The average $n(r)$ is 4.50. It means that bulk water was in a form of liquid water. A snapshot of tetrahedral structure shows water 4 and 5 molecules surrounding water in the center see in Figure 11c. When water molecules are confined in nanotubes, their configurations differ from those in the bulk phase. Water molecules try to position themselves into shells inside the pores. For the (9,9) nanotube, all the water molecules are located close to the wall of the nanotube and the highest distribution of the coordination number is 4. The reason for the coordination of water molecules in the (9,9) nanotube being less than that in bulk water is the interactions between water molecules and the nanotube wall. These strong interactions combine with very limited space result in decreasing the number of water molecules that interact with one another. It seems that water behaves as the ice-like

structure. A cross section of a snapshot illustrates that water formed the single hexagonal ring inside (9,9)-nanotubes (see Figure 12a (*right*)).

In larger nanotubes, (10,10) SWCNTa, -SWCNTb and –SWBNNT, the major $n(r)$ distribution are 5 and 4 with the average $n(r)$ of 4.84 (SWCNTa), 4.79 (SWCNTb) and 4.79 (SWBNNT). Most of the water molecules in the middle of the pore are supposed to have a coordination number equal to 5, while the water molecules that locate close to the pore wall have a coordination number equal to 4. The trend of the ratio between the coordination numbers 4 and 5 is found to increase with increasing the nanotube size (see Figure 12(b-f)). This means that when the size of the nanotube increases, the water molecules will behave in the same way as in the bulk phase. However, the ratio between the coordination numbers 4 and 5 in the (10,10) nanotube is quite high. This probably results from the large amount of water molecules close to the wall. A cross section snapshot shows a single ring and near the tube wall and a water column at the center of nanotube. Its coordination number was in the range of liquid. This result indicating that the water confined in (10,10)-nanotubes have structural properties in between ice and liquid water properties. For the wider diameters, (12,12), (14,14), (16,16) and (20,20)-SWCNTa,-SWCNTb and –SWBNNT, the maximum $n(r)$ distribution is 5, following with 4, 6, 3, 8. The average $n(r)$ distribution indicated the liquid water structure.

Although the $n(r)$ distributions of water inside (10,10), (12,12), (14,14), (16,16) and (20,20) nanotubes were similar, the different arrangements were observed (inset snapshots in Figure 12 (*right*)). In the largest nanotube (20,20), confirmed water appeared to be bulk water character. In smaller tubes, (12,12) and (14,14) multi-layer of concentric rings can be observed from snapshots in Figure 12.

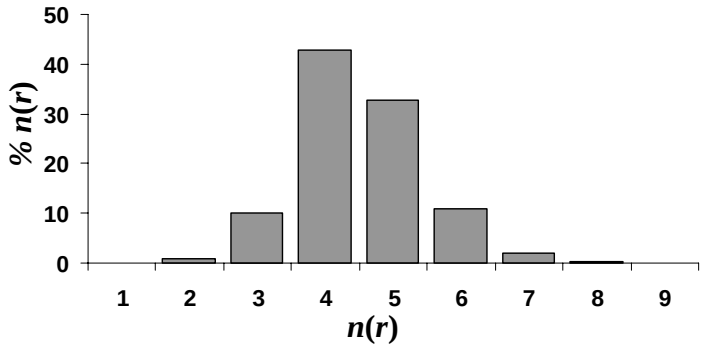

(a) Histogram of percentage $n(r)$ distribution of bulk water

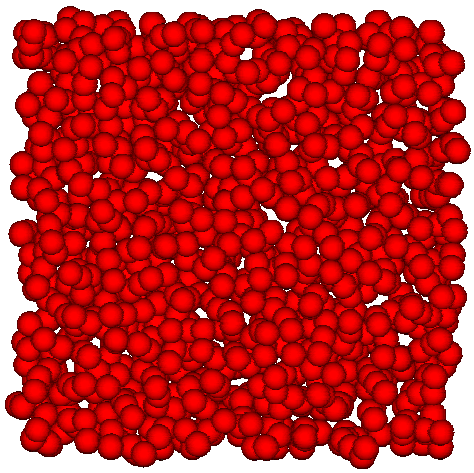

(b) A snapshot of bulk water

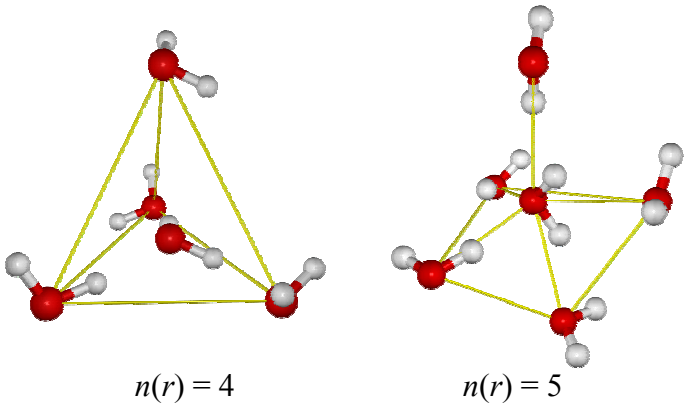

(c) Snapshot of tetrahedral structures

Figure 11 Structure of coordination number distribution of bulk water

a) Histogram of percentage $n(r)$ distribution of bulk water

b) A snapshot of bulk water

c) Snapshot of tetrahedral structures

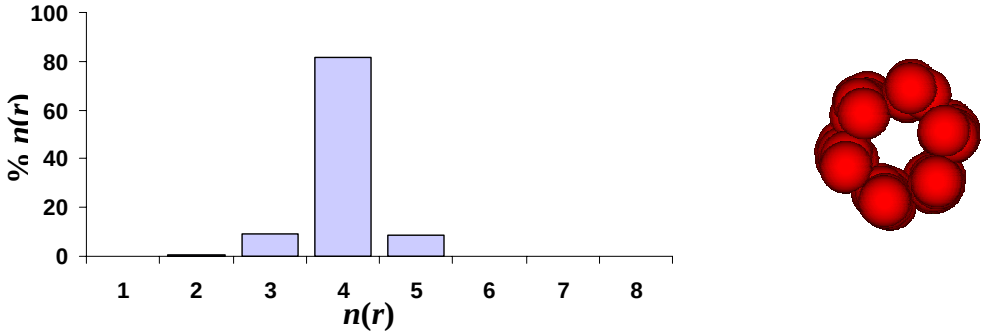

(a) water 77 molecules in (9,9)-SWBNNT

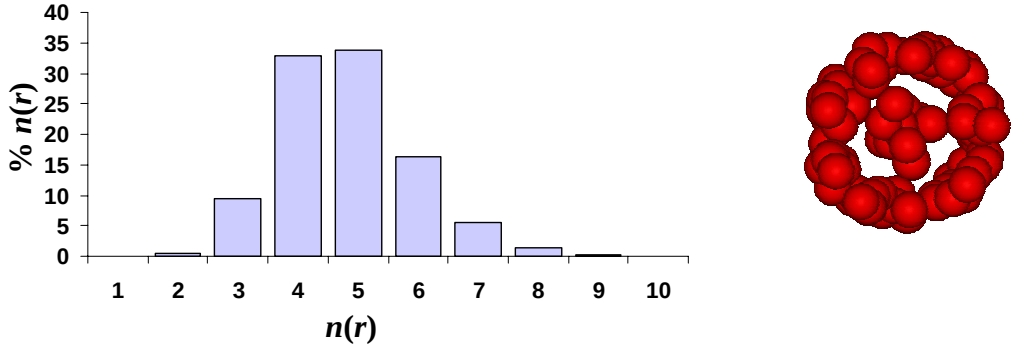

(b) water 102 molecules in (10,10)-SWBNNT

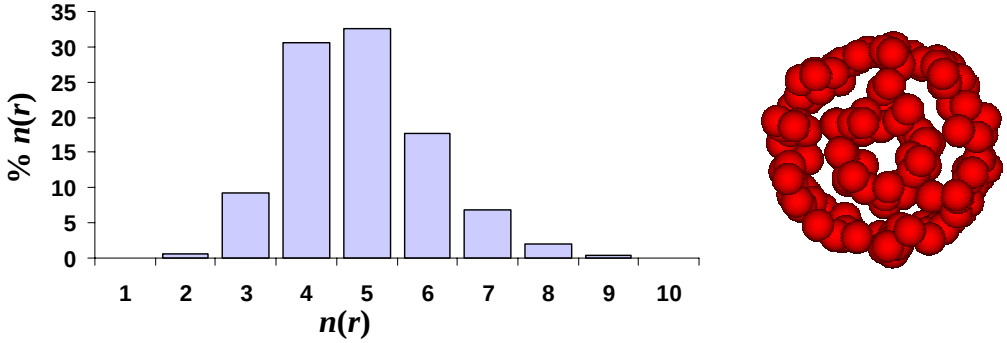

(c) water 162 molecules in (12,12)-SWBNNT

Figure 12 Histogram of coordination number distribution of water in SWBNNT (*left*) and inset cross section snapshots (*right*).

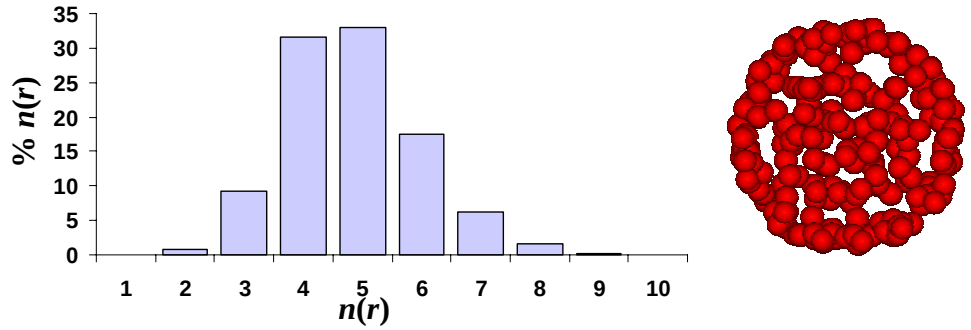

(d) water 237 molecules in (14,14)-SWBNNT

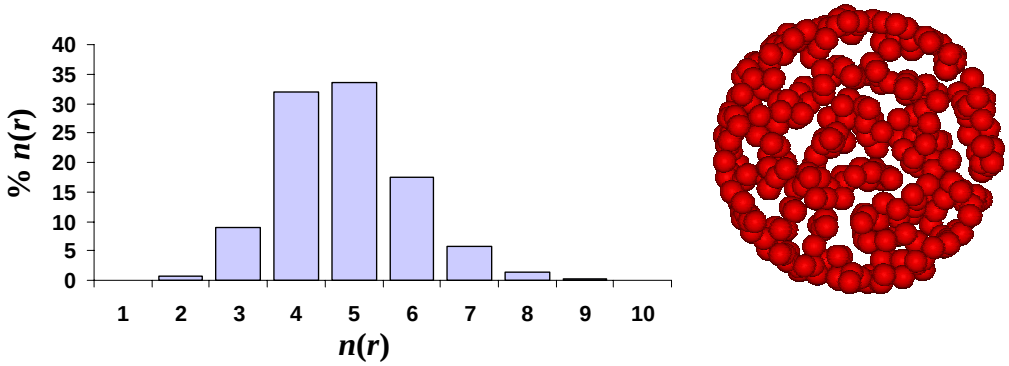

(e) water 327 molecules in (16,16)-SWBNNT

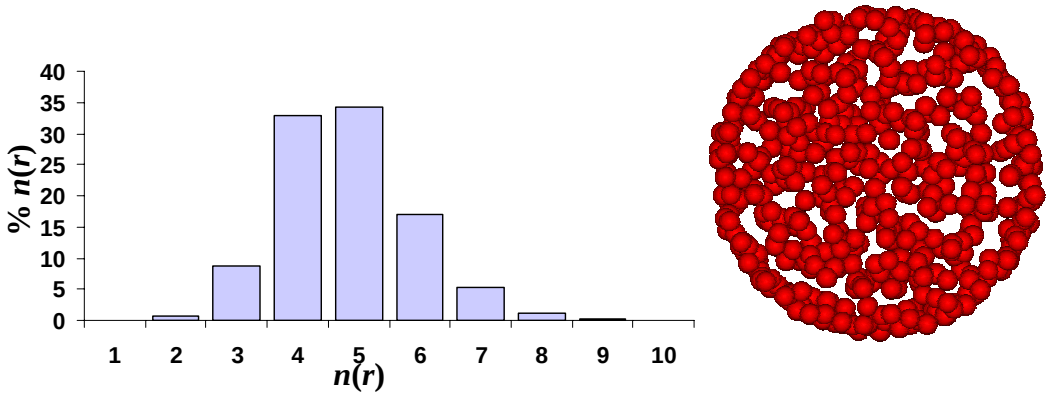

(f) water 547 molecules in (20,20)-SWBNNT

Figure 12 Histogram of coordination number distribution of water in SWBNNT (*left*) and inset cross section snapshots (*right*). (Cont'd)

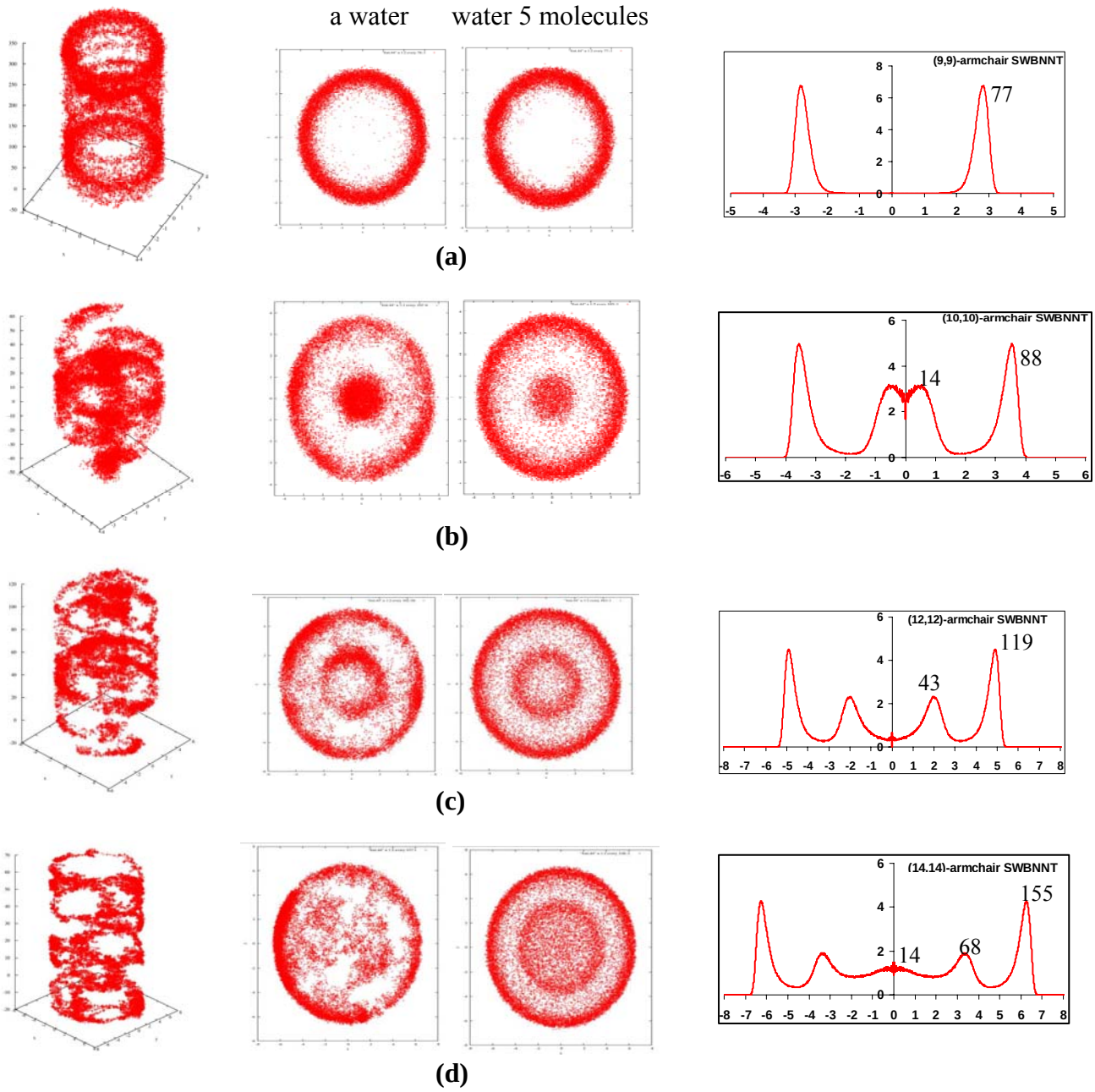

Figure 13 Three-dimensional distribution trajectories (*left*) of a selected water molecule in (9,9)- **(a)**, (10,10)- **(b)**, (12,12)- **(c)**, (14,14)- **(d)**, (16,16)- **(e)** and (20,20)- **(f)** armchair SWBNNTs; their projections onto the *xy* plane (*middle*); and cylindrical $g(r)$ distribution functions of water with respect to the center of those SWBNNTs (*right*).

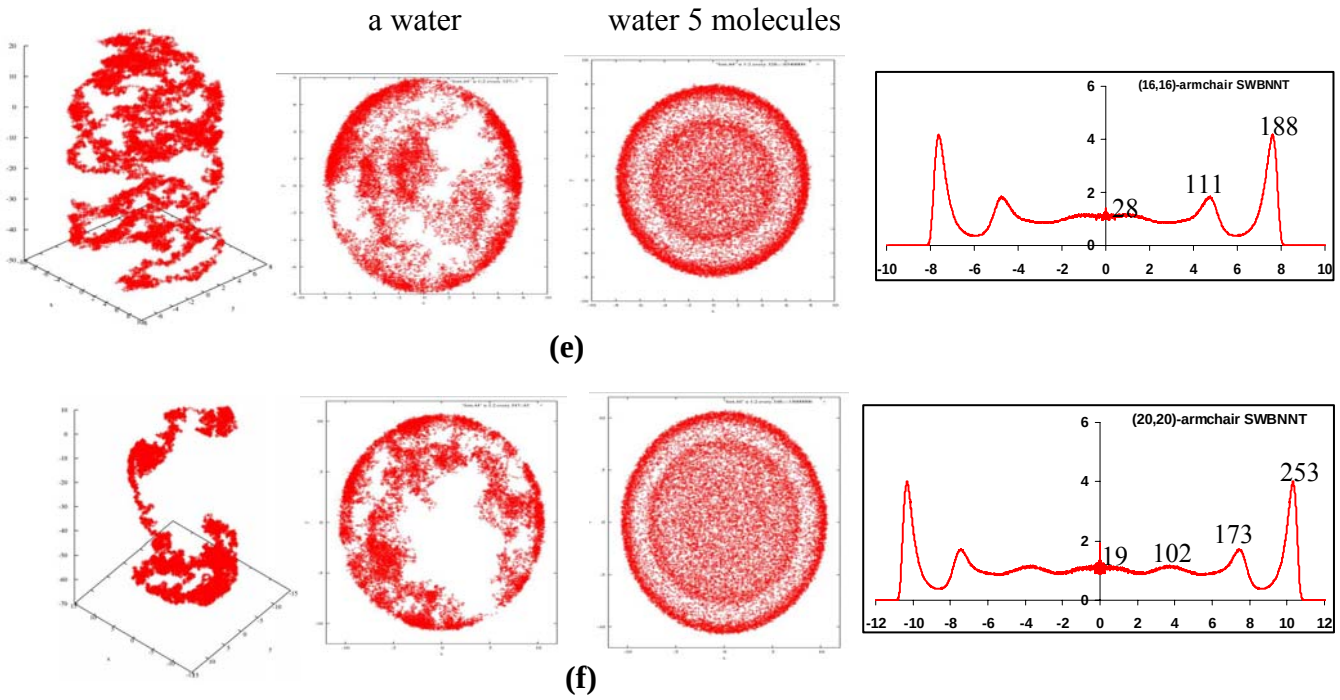

Figure 13 Three-dimensional distribution trajectories (*left*) of a selected water molecule in (9,9)- **(a)**, (10,10)- **(b)**, (12,12)- **(c)**, (14,14)- **(d)**, (16,16)- **(e)** and (20,20)- **(f)** armchair SWBNNTs; their projections onto the *xy* plane (*middle*); and cylindrical $g(r)$ distribution functions of water with respect to the center of those SWBNNTs (*right*). (cont'd)

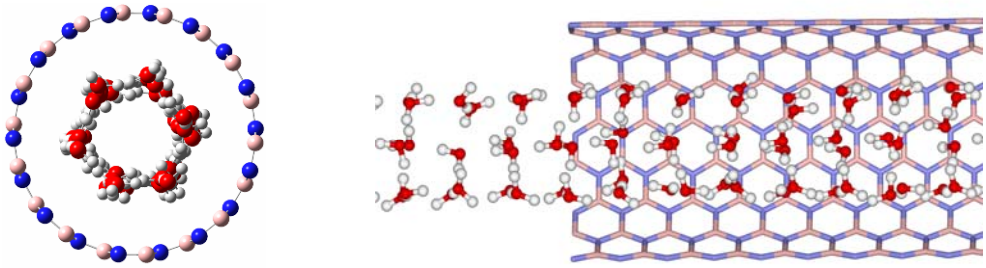

(a) **(b)**

Figure 14 Top view **(a)** and side view **(b)** of a snapshot of the six-membered ring structure of the single-walled ice-like nanotube in a (9,9)-armchair SWBNNTs.

Figures 13(a-f) show on right hand side, the cylindrical $g(r)$-functions across the boron-nitride nanotubes. The numbers above the curves refer to the average number of water molecules present in the various regions; the total number of molecules is listed in Table 1. The left hand side of the figures gives a visual impression by showing, at regular time intervals, x and y-coordinates of a one (*left*) and five (*right*) water molecules during the simulations. It shows that, except in the narrowest tube ((9,9)-nanotubes), where there is not enough space, molecules exchange frequently between the boundary layer and the inside of the tube.

The functions for the other two cases, SWCNTa and SWCNTb, are very similar to Figure 13(a-f) and are therefore not shown here. The boundary-layer peaks are slightly enhanced with increasing wall-water interactions, as expected. As an example, this work find an average of 250, 252, and 254 water molecules in the boundary layer in the cases SWCNTa, SWCNTb, and SWBNNT, respectively.

The cylindrical RDF of water molecules inside the nanotube obviously shows shell like configurations. In the (9,9) nanotube, most water molecules locate close to the wall and there is no water molecule located in the middle of the pore. This results from the attractive interactions between water molecules and the pore wall.

For the wider nanotube pore sizes, some water molecules still locate close to the pore wall and the excess water molecules form a ring like structure in the middle of pores. In the (10, 10) nanotube, the cylindrical RDF shows two maximum peaks. The distance between the two maximum peaks is 3.00 Å, which is significantly higher than that in the (12,12), (14,14), (16,16) and (20,20): (2.89, 2.89, 2.91 and 2.92 Å, respectively). These may result from the attraction between the water molecules in the middle of the pore in the (10,10) nanotube. Moreover, it was also found that there is less water exchange between the layers in the (10,10) nanotube and the exchange increases when the pore sizes increase.

Figures 13e and 13f show that above a diameter of about 18 Å the water density at the center is close to bulk density, about 1 g cm^{-3}. In narrower tubes, Figures 13b, 13c and 13d, the wall-induced layering leads to oscillations of the water density extending to the center. In the narrowest tube, Figure 13a, there is space for just one layer of water next to the wall, and the density at the center is negligible, in keeping with the results by Mashl et al. (Mashl *et al.*, 2003) for their (9,9) single wall nanotube.

Furthermore, the strong attractive interactions induced water molecules form the ice-like single-shell hexagonal structure inside the (9,9)-nanotubes (SWCNTa, SWCNTb and SWBNNT) as showed in Figure 14, it is similar to previous work (Marshl *et al.*, 2003).

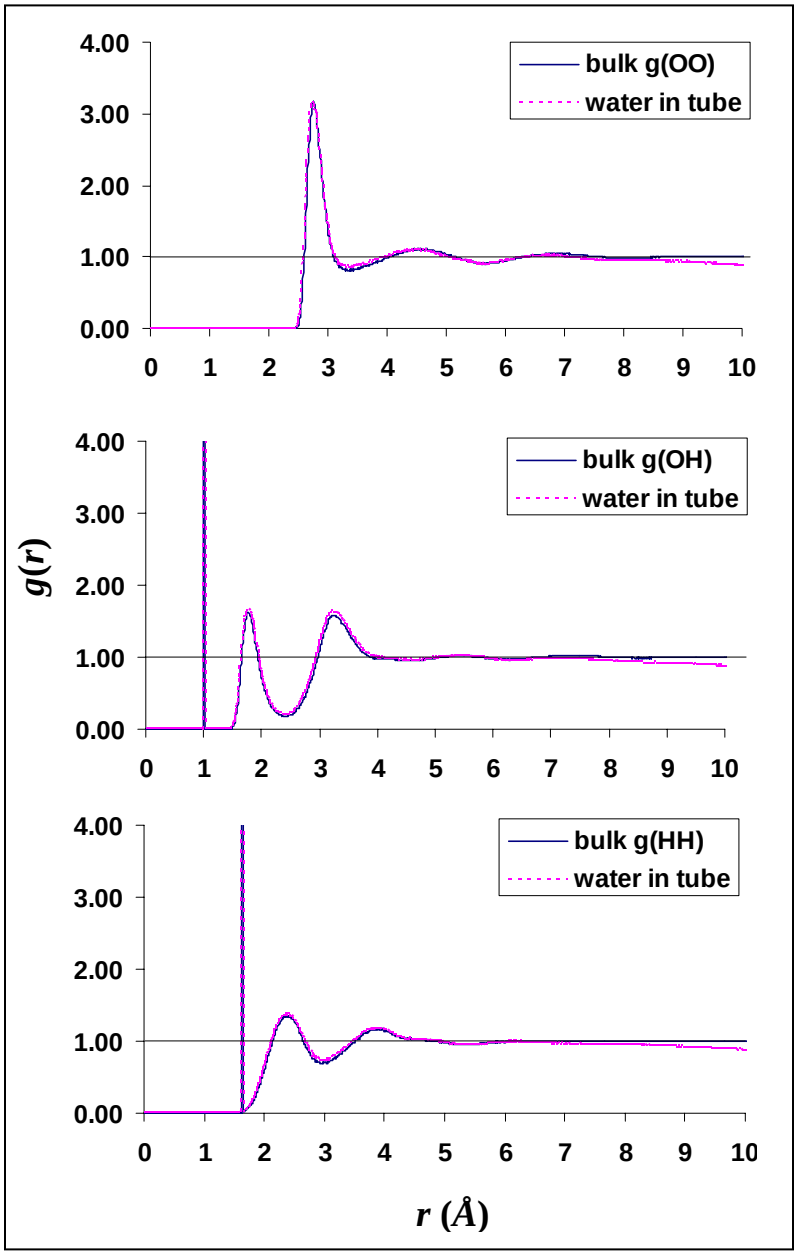

Figure 15 Radial distribution functions g_{OO}, g_{OH}, and g_{HH} for pure water (solid) and for water molecules in the center (-2.2 Å < r < 2.2 Å) of the (20,20) SWBNNT (dashed).

In order to further analyze the water structure in the center of a large tube, Figure 15 compares the three radial distribution functions (rdf) g_{OO}, g_{OH}, and g_{HH} obtained in pure bulk water reference run with ones obtained for molecules in the center of the (20,20)-SWBNNT. Only sites inside a cylinder of 2.2 Å radius around the *z*-axis are selected as centers for these function. Since the number density ρ_b is not constant, the normalization of these functions is somewhat arbitrary. The zone of constant density inside the tube is about 8 Å wide, this case thus selected to set $g(r \approx 6\,\text{Å}) = 1$. The Figure 15 shows that all three g-functions inside the tube are almost indistinguishable from the bulk ones. Thus, even with the strongest of the three wall-water interaction models, the water inside the tube is structurally very close to bulk water.

Dynamics and diffusions of bulk water molecules and water molecules enclosed in different sizes of nanotubes

Dynamic properties of water were expressed in terms of its self-diffusion coefficient that obtained from slope of average mean square displacement (MSD) of water molecules. MSD curves show in Figure 17 (bulk system) and Figure 18 (water in confined systems).

Figure 16 shows the decay of the number of water molecules present in the boundary layer of the tube wall (defined as the water molecules with $r = \sqrt{x^2 + y^2}$ -values larger than the minima in the distribution functions shown in Figure 13(a - f) at an initial time t_0, as a function of time. This figure shows, as examples, the results for large and a small tubes and also for different interactions strengths (hydrophobicities) between water and wall. The long time limit of these functions is the expectation value of the initial molecules being present in the boundary layer when the system is totally mixed. It is seen that this value is reached in all cases after about 150 ps. Functions of type

$$f(t) = a + b * \exp(-t / \tau)$$

describe the correlation very well in all cases, the correlation times τ are all between 40 and 50 ps with the higher values for the stronger wall-water interactions. The sum $a + b$ is close to the average total number of water molecules present in the boundary layer, which is also reported in Figure 13(a-f) from integrations of the distribution functions plotted there.

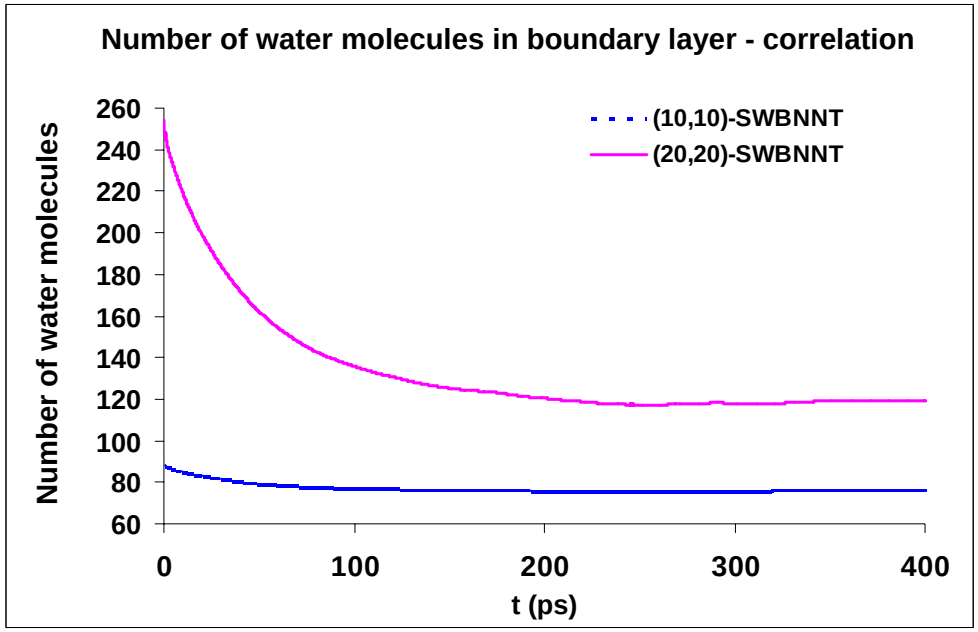

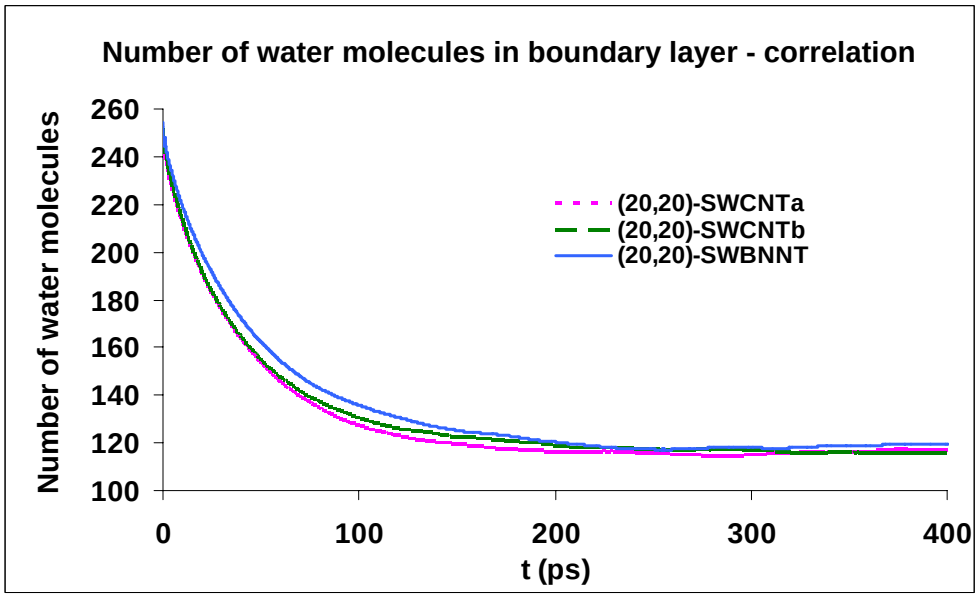

Figure 16 Average number of water molecules present in the first water layer next to the pore wall at time 0 and still present there at later times, from simulations (10,10)-SWBNNT and (20,20)-SWBNNT (*top*), and additionally, for comparison, SWCNTa and SWCNTb (*bottom*).

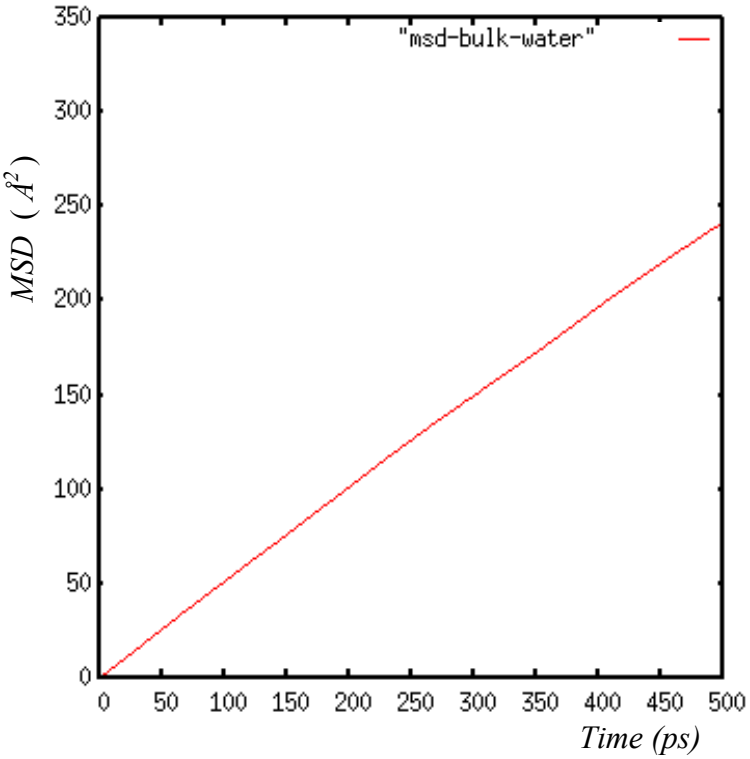

Figure 17 Axial mean square displacement (*MSD*) (z axis) of bulk water (1,000 molecules).

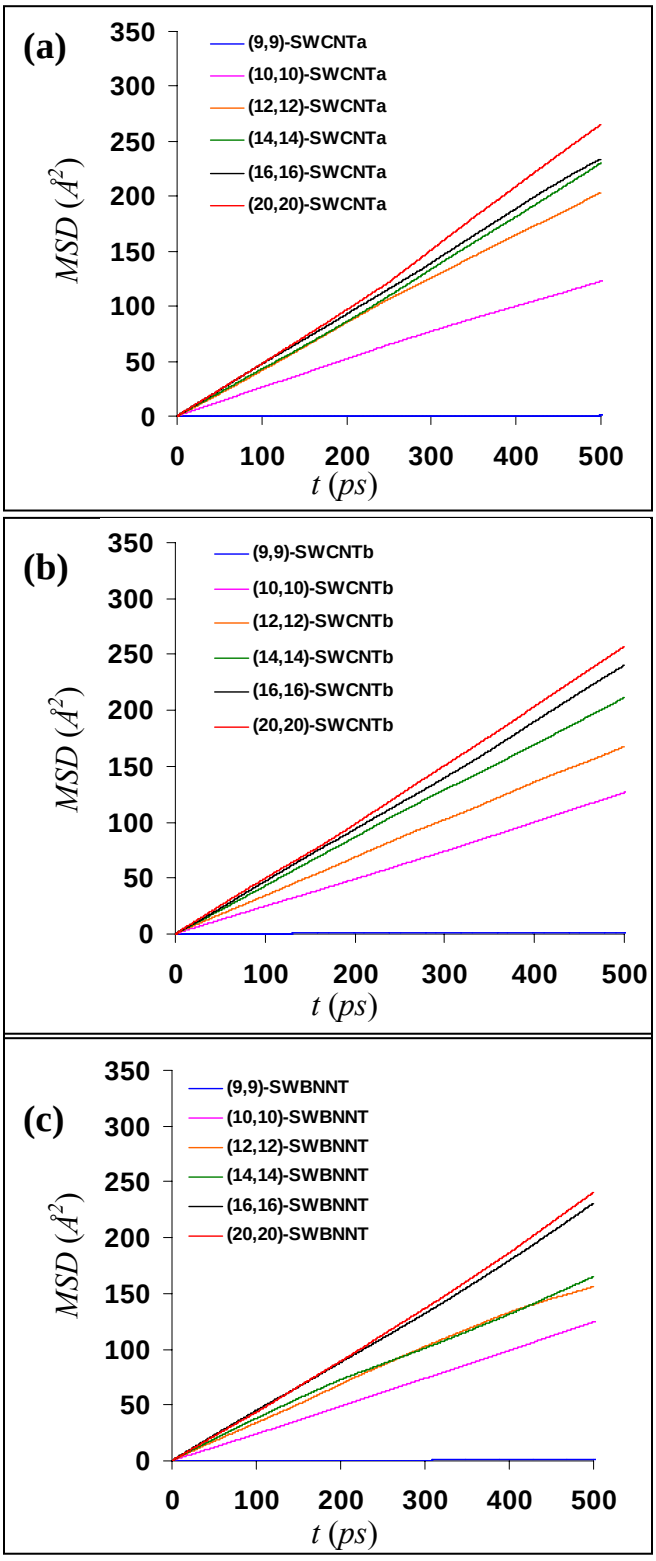

Figure 18 Mean square displacements of the oxygen atom, from simulations SWCNTa **(a)**, SWNCNTb **(b)**, and SWBNNT **(c)**. Self-diffusion coefficients see Table 5 and Figure 19.

Table 5 Axial self-diffusion coefficients ***Dz*** (cm^2/s) of water in nanotubes at the average temperature of 298 K and the water density of 1.00 g cm^{-3}. The uncertainties are estimated to be of the order of $\pm 0.10\ cm^2\ s^{-1}$

Model	***Dz*** **(**$cm^2\ s^{-1}$**)**	**Model**	***Dz*** **(**$cm^2\ s^{-1}$**)**	**Model**	***Dz*** **(**$cm^2\ s^{-1}$**)**
Bulk water	2.50×10^{-5}				
					ε_{BO}=0.11433
εij (Kcal mol^{-1})	ε_{CO}=0.11433		ε_{CO}=0.11433		ε_{NO}=0.11433
(9,9)- SWCNTa	3.00×10^{-8}	(9,9)- SWCNTb	9.80×10^{-8}	(9,9)- SWBNNT	8.55×10^{-8}
(10,10)- SWCNTa	1.20×10^{-5}	(10,10)- SWCNTb	1.30×10^{-5}	(10,10)- SWBNNT	1.50×10^{-5}
(12,12)- SWCNTa	2.05×10^{-5}	(12,12)- SWCNTb	1.70×10^{-5}	(12,12)- SWBNNT	1.60×10^{-5}
(14,14)- SWCNTa	2.30×10^{-5}	(14,14)- SWCNTb	2.10×10^{-5}	(14,14)- SWBNNT	1.60×10^{-5}
(16,16)- SWCNTa	2.35×10^{-5}	(16,16)- SWCNTb	2.40×10^{-5}	(16,16)- SWBNNT	2.40×10^{-5}
(20,20)- SWCNTa	2.70×10^{-5}	(20,20)- SWCNTb	2.60×10^{-5}	(20,20)- SWBNNT	2.50×10^{-5}

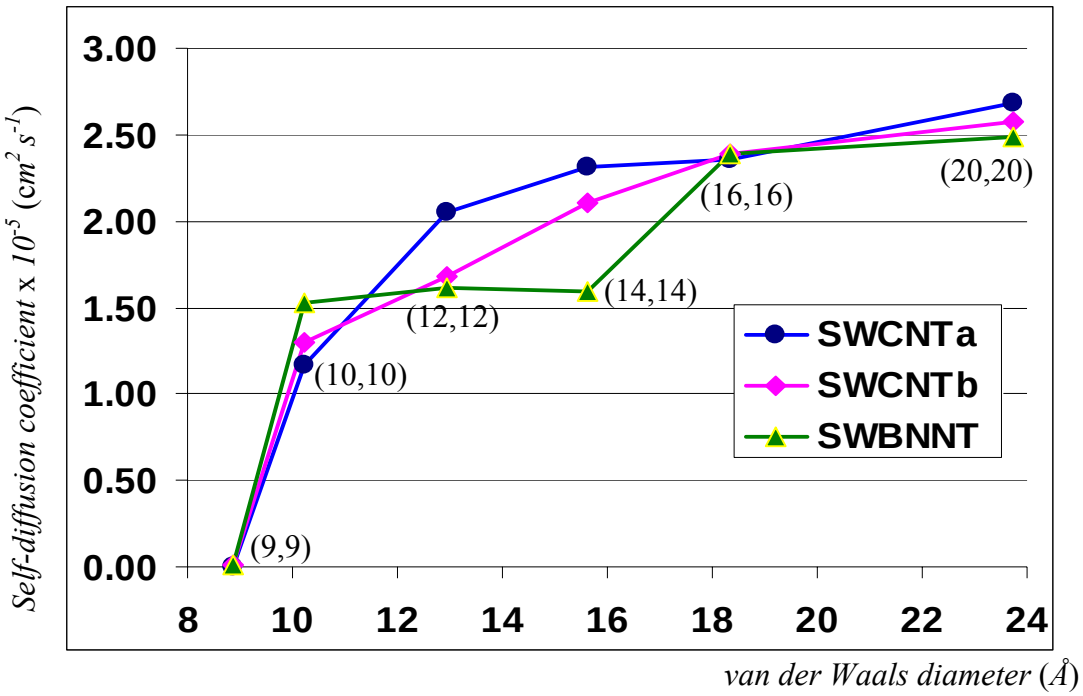

Figure 19 Comparison self-diffusion coefficients of water confined in 3 difference attractive interactions and difference size nanotube.

The Figure 18 shows the averaged mean-square displacements of the water molecules, corrected for the drifts induced by the thermostat, for all systems. The translational self-diffusion coefficients reported in Table 5 and Figure 19 have been obtained by fitting expressions

$$< (z - z_0)^2(t) >= A + 2D_z \cdot t$$

to the mean-square displacement curves in z-direction at long times. This work obtained a value of $D = 2.5 \pm 0.1 \cdot 10^{-5}$ $\mathrm{cm}^2\,\mathrm{s}^{-1}$ from the pure water simulation. This D-value is intermediate between the values reported by Marshl ($2.69 \cdot 10^{-5}\,\mathrm{cm}^2\,\mathrm{s}^{-1}$) and by experimental diffusion coefficient of water ($2.35 \cdot 10^{-5}\,\mathrm{cm}^2\,\mathrm{s}^{-1}$) (Lide, 1995). In passing, here also take good note of the remarks in these papers that the fact that the experimental D is well reproduced by a given model for the pure liquid at a given state point does not necessarily mean that it will also do so in solutions, at an interface, or under different thermodynamic conditions. This work nevertheless expects systematic trends (e.g. size dependences, or when the wall-water interactions are modified) to be reasonably well mirrored.

Figure 19 shows that no self-diffusion can be detected in the narrowest tubes during the simulation runs of a few nanoseconds. D_z increases with increasing tube diameter and reaches its bulk value in the widest tubes with diameters of about 24 Å, the convergence being faster for smaller wall-water interactions. In the case of the boron-nitride tubes the convergence is not monotonous. These systems were not able to distinguish particular structural features that may explain the plateau between (10,10) and (14,14) tubes (which here is outside uncertainties) in a convincing way. Even larger irregular variations of the self-diffusion have been observed by Liu *et al.* (Liu *et al.*, 2005) in narrower CNTs. No influence of the wall-water interactions can be distinguished in tubes wider than about 20 Å.

It is seen in Figure 19 that in almost all cases the linear regime of the mean-square displacement is reached after about 10 ps. Comparing this time with the correlation time for water molecules staying in the boundary layer discussed above (see Figure 16), viz. about 40 to 50 ps, indicates that a separation of the total diffusion into a component originating in the boundary layer molecules and a second one originating in the bulk would be justified.

In all cases, the self-diffusion coefficients increase as the nanotube diameters increase. In the case of the small diameter (9,9) nanotubes, the water shows anomalous ice-like behavior in both ice coordination number and very slow flow of 3 order less than that seen in bulk and the large-nanotubes, while a liquid-like degree of water-water hydrogen bonding.

For the wider pore (12,12), (14,14), (16,16) and (20,20) nanotubes, the axial self-diffusion coefficients increase as the pore increase and reach that to the bulk water. The diffusion is sensitive to the $\varepsilon_{C\text{-}O}$ van der Waals attractive interaction (LJ potential). The simulations of water in SWCNTa and SWCNTb represented the smooth attractive interactions; the small energy interaction ($\varepsilon c\text{-}o$ = 0.1143 kcal mol^{-1}) gives the large self-diffusion coefficients while the higher interaction ($\varepsilon c\text{-}o$ = 0.1230 kcal mol^{-1}) gives smaller self-diffusion coefficients.

CONCLUSIONS

MD simulations were used to study the molecular distributions and transport properties of water confined in nanotubes with difference of pore diameters and attractive interactions between wall and water. Water motions and orientations can be modified by confining in single-walled nanotubes. In the (9,9)-armchair nanotubes, water adopts a six-membered ring ice-like structure. The distribution structure of water confined in nano-space is not homogeneous. The larger diameter nanotubes, multi-layering of water occur, where water behaves like bulk water in the inner layers. Water molecules can freely exchange between inner and outer layers. Self-diffusion coefficient of water increases as the nanotube diameter increases. The attractive interactions between water and nanotube wall is a key role of water diffusivity. Small changes in the water-wall interaction can lead to changes in the axial diffusion of water in nanotubes at identical sizes. The axial diffusion of water in the SWCNTa and SWCNTb are faster than that in the SWBNNT ((12,12)-(20,20)-nanotubes), the strong attractive interactions (water and tube wall) impose the slower diffusion of water.

LITERATURE CITED

Bai, J., J. Wang and X.C. Zeng. 2006. Multiwalled ice helixes and ice nanotubes. **Proceedings of the National Academy of Sciences of the United States of America** 103(52):19664-19667.

Behler, J., D.W. Price and M.G.B. Drew. 2001. Water structuring properties of carbohydrates, molecular dynamics studies on 1,5-anhydro-D-fructose. **Physical Chemistry Chemical Physics** 3(4):588-601.

Berendsen, H.J.C., J.R. Grigera and T.P. Straatsma. 1987. The missing term in effective pair potentials. **Journal of Physical Chemistry** 91(24):6269-6271.

Berezhkovskii, A. and G. Hummer. 2002. Single-File Transport of Water Molecules through a Carbon Nanotube. **Physical Review Letters** 89(6):064503/064501-064503/064504.

Bianco, A., K. Kostarelos and M. Prato. 2005. Applications of carbon nanotubes in drug delivery. **Current Opinion in Chemical Biology** 9(6):674-679.

Chou, C.-C., H.-Y. Hsiao, Q.-S. Hong, C.-H. Chen, Y.-W. Peng, H.-W. Chen and P.-C. Yang. 2008. Single-Walled Carbon Nanotubes Can Induce Pulmonary Injury in Mouse Model. **Nano Letters** 8(2):437-445.

Golberg, D., Y. Bando, K. Kurashima and T. Sato. 2000. MoO3-promoted synthesis of multi-walled BN nanotubes from C nanotube templates. **Chemical Physics Letters** 323(1,2):185-191.

Guillot, B. 2002. A Reappraisal of what we have learnt during three decades of computer simulations on water. **Journal of Molecular Liquids** 101(1-3):219-260.

Head-Gordon, T. and M.E. Johnson. 2006. Tetrahedral structure or chains for liquid water. **Proceedings of the National Academy of Sciences of the United States of America** 103(21):7973-7977.

Hummer, G., J.C. Rasaiah and J.P. Noworyta. 2001. Water conduction through the hydrophobic channel of a carbon nanotube. **Nature** 414(6860):188-190.

Iijima, S. 1991. Helical microtubules of graphitic carbon. **Nature** 354(6348):56-58.

Iijima, S. and T. Ichihashi. 1993. Single-shell carbon nanotubes of 1-nm diameter. **Nature** 363:603-605.

Ishigami, M., S. Aloni and A. Zettl. 2003a. Properties of boron nitride nanotubes. **American Institute of Physics Conference Proceedings** 696 (Scanning Tunneling Microscopy/Spectoscopy and Related Techniques):94-99.

Ishigami, M., S. Aloni and A. Zettl. 2003b. Scanning tunneling microscopy and spectroscopy of boron nitride nanotubes. **American Institute of Physics Conference Proceedings Conference Proceedings** 685 (Molecular Nanostructures):389-393.

Joseph, S. and N.R. Aluru. 2008. Why Are Carbon Nanotubes Fast Transporters of Water? **Nano Letters** 8(2):452-458.

Kalra, A., S. Garde and G. Hummer. 2003. Osmotic water transport through carbon nanotube membranes. **Proceedings of the National Academy of Sciences of the United States of America** 100(18):10175-10180.

Kalra, A., G. Hummer and S. Garde. 2004. Methane Partitioning and Transport in Hydrated Carbon Nanotubes. **Journal of Physical Chemistry B** 108(2):544-549.

Koga, K., G.T. Gao, H. Tanaka and X.C. Zeng. 2001. Formation of ordered ice nanotubes inside carbon nanotubes.**Nature** 412(6849):802-805.

Koga, K., R.D. Parra, H. Tanaka and X.C. Zeng. 2000a. Ice nanotube: What does the unit cell look like? **Journal of Chemical Physics** 113(12):5037-5040.

Koga, K. and H. Tanaka. 2005. Phase diagram of water between hydrophobic surfaces. **Journal of Chemical Physics** 122(10):104711.

Koga, K., H. Tanaka and X.C. Zeng. 2000b. First-order transition in confined water between high-density liquid and low-density amorphous phases. **Nature** 408(6812):564-567.

Kolesnikov, A.I., J.-M. Zanotti, C.-K. Loong, P. Thiyagarajan, A.P. Moravsky, R.O. Loutfy and C.J. Burnham. 2004. Anomalously Soft Dynamics of Water in a Nanotube: A Revelation of Nanoscale Confinement. **Physical Review Letters** 93(3):035503/035501-035503/035504.

Kuhs, W.F., J.L. Finney, C. Vettier and D.V. Bliss. 1984. Structure and hydrogen ordering in ices VI, VII, and VIII by neutron powder diffraction. **Journal of Chemical Physics** 81(8):3612-3623.

Li, J., X. Gong, H. Lu, D. Li, H. Fang and R. Zhou. 2007. Electrostatic gating of a nanometer water channel. **Proceedings of the National Academy of Sciences of the United States of America** 104(10):3687-3692.

Li, L., D. Bedrov and G.D. Smith. 2006. Water-Induced Interactions between Carbon Nanoparticles. **Journal of Physical Chemistry B** 110(21):10509-10513.

Lide, D. R., Ed. 1995. **Handbook of Chemistry and Physics.** CRC Boca Raton, FL.

Liu, Y. and S. Consta. 2005. Dynamic breaking and restoring of finite water chains inside carbon nanotubes. **Computing Letters** 1(4):192-197.

Liu, Y. and Q. Wang. 2005. Transport behavior of water confined in carbon nanotubes. **Physical Review B: Condensed Matter and Materials Physics** 72(8):085420/085421-085420/085424.

Liu, Y., Q. Wang, T. Wu and L. Zhang. 2005a. Fluid structure and transport properties of water inside carbon nanotubes. **Journal of Chemical Physics** 123(23):234701/234701-234701/234707.

Liu, Y., Q. Wang, L. Zhang and T. Wu. 2005b. Dynamics and Density Profile of Water in Nanotubes as One-Dimensional Fluid. **Langmuir** 21(25):12025-12030.

Malek, K. and M.-O. Coppens. 2003. Knudsen self- and Fickian diffusion in rough nanoporous media. **Journal of Chemical Physics** 119(5):2801-2811.

Mann, D.J. and M.D. Halls. 2003. Water Alignment and Proton Conduction inside Carbon Nanotubes. **Physical Review Letters** 90(19):195503/195501-195503/195504.

Marti, J. and M.C. Gordillo. 2001a. Temperature effects on the static and dynamic properties of liquid water inside nanotubes. **Physical Review E: Statistical, Nonlinear, and Soft Matter Physics** 64(2-1):021504/021501-021504/021506.

Marti, J. and M.C. Gordillo. 2001b. Time-dependent properties of liquid water isotopes adsorbed in carbon nanotubes. **Journal of Chemical Physics** 114(23):10486-10492.

Marti, J. and M.C. Gordillo. 2002. Microscopic dynamics of confined supercritical water. **Chemical Physics Letters** 354(3,4):227-232.

Marti, J. and M.C. Gordillo. 2003. Structure and dynamics of liquid water adsorbed on the external walls of carbon nanotubes. **Journal of Chemical Physics** 119(23):12540-12546.

Mashl, R.J., S. Joseph, N.R. Aluru and E. Jakobsson. 2003. Anomalously Immobilized Water: A New Water Phase Induced by Confinement in Nanotubes. **Nano Letters** 3(5):589-592.

Meyyappan, M., Ed. 2005. **Carbon nanotubes: Science and applications**. Boca Raton, CRC Press LLC

Mukherjee, B., P.K. Maiti, C. Dasgupta and A.K. Sood. 2007a. Strong correlations and Fickian water diffusion in narrow carbon nanotubes. **Journal of Chemical Physics** 126(12):124704/124701-124704/124708.

Mukherjee, B., K. Maiti Prabal, C. Dasgupta and A.K. Sood. 2007b. Structure and dynamics of confined water inside narrow carbon nanotubes. **Journal of Nanoscience and Nanotechnology** 7(6):1796-1799.

Noy, A., H.G. Park, F. Fornasiero, J.K. Holt, C.P. Grigoropoulos and O. Bakajin. 2007. Nanofluidics in carbon nanotubes. **Nano Today** 2(6):22-29.

Smith, W.T. R. Forester, I. T. Todorov and M. Leslie. 2006. The DL_POLY 2.0, User Manual, CCLRC, Daresbury Laborator Daresbury, UK, Version 2.17.

Soper, A.K. 2000. The radial distribution functions of water and ice from 220 to 673 K and at pressures up to 400 MPa. **Chemical Physics** 258(2-3):121-137.

Striolo, A. 2006. The Mechanism of Water Diffusion in Narrow Carbon Nanotubes. **Nano Letters** 6(4):633-639.

Striolo, A., A.A. Chialvo, P.T. Cummings and K.E. Gubbins. 2003. Water Adsorption in Carbon-Slit Nanopores. **Langmuir** 19(20):8583-8591.

Striolo, A., A.A. Chialvo, P.T. Cummings and K.E. Gubbins. 2006. Simulated water adsorption in chemically heterogeneous carbon nanotubes. **Journal of Chemical Physics** 124(7):074710/074711-074710/074711.

Striolo, A., P.T. Cummings, A.A. Chialvo and K.E. Gubbins. 2004a. Adsorption and diffusion of water in activated carbon nanopores. **Advances in Science and Technology (Faenza, Italy)** 42 (Computational Modeling and Simulation of Materials III, Part A):531-540.

Striolo, A., K.E. Gubbins, A.A. Chialvo and P.T. Cummings. 2004b. Simulated water adsorption isotherms in carbon nanopores. **Molecular Physics** 102(3):243-251.

Sui, H., B.G. Han, J.K. Lee, P. Walian and B.K. Jap. 2001. Structural basis of water-specific transport through the AQP1 water channel. **Nature** 414(6866):872-878.

Supple, S. and N. Quirke. 2003. Rapid Imbibition of Fluids in Carbon Nanotubes. **Physical Review Letters** 90(21):214501/214501-214501/214504.

Supple, S. and N. Quirke. 2004. Molecular dynamics of transient oil flows in nanopores I: imbibition speeds for single wall carbon nanotubes. **Journal of Chemical Physics** 121(17):8571-8579.

Supple, S. and N. Quirke. 2005. Molecular dynamics of transient oil flows in nanopores. Part 2. Density profiles and molecular structure for decane in carbon nanotubes. **Journal of Chemical Physics** 122(10):104706/104701-104706/104708.

Tajkhorshid, E., P. Nollert, O. Jensen Morten, J.W. Miercke Larry, J. O'Connell, M. Stroud Robert and K. Schulten. 2002. Control of the selectivity of the aquaporin water channel family by global orientational tuning. **Science** 296(5567):525-530.

Takaiwa, D., K. Koga and H. Tanaka. 2007. Structures of filled ice nanotubes inside carbon nanotubes. **Molecular Simulation** 33(1-2):127-132.

Waghe, A., J.C. Rasaiah and G. Hummer. 2002. Filling and emptying kinetics of carbon nanotubes in water. **Journal of Chemical Physics** 117(23):10789-10795.

Wang, Z.L., P. Poncharal and W.A. De Heer. 2000. Measuring physical and mechanical properties of individual carbon nanotubes by in situ TEM. **Journal of Physics and Chemistry of Solids** 61(7):1025-1030.

Won, C.Y. and N.R. Aluru. 2007. Water Permeation through a Subnanometer Boron Nitride Nanotube. **Journal of the American Chemical Society** 129(10):2748-2749.

Won, C.Y. and N.R. Aluru. 2008. Structure and Dynamics of Water Confined in a Boron Nitride Nanotube. **Journal of Physical Chemistry C** 112(6):1812-1818.

Yang, L. and S. Garde. 2007. Modeling the selective partitioning of cations into negatively charged nanopores in water. **Journal of Chemical Physics** 126(8):084706/084701-084706/084708.

Zou, J., B. Ji, X.-Q. Feng and H. Gao. 2006a. Molecular-dynamic studies of carbon-water-carbon composite nanotubes. **Small** 2(11):1348-1355.

Zou, J., B. Ji, X.-Q. Feng and H. Gao. 2006b. Self-Assembly of Single-Walled Carbon Nanotubes into Multiwalled Carbon Nanotubes in Water: Molecular Dynamics Simulations. **Nano Letters** 6(3):430-434.

APPENDICES

Appendix A

Data support

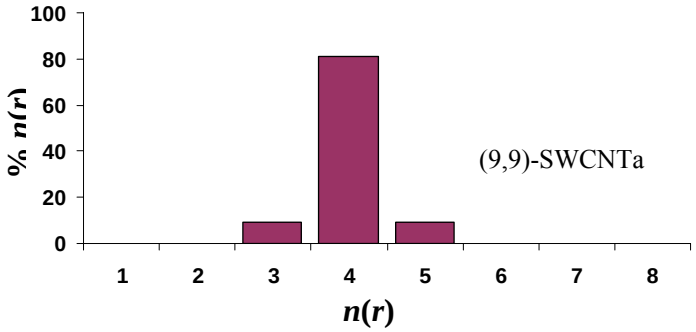

(a) water 77 molecules in (9,9)-SWCNTa

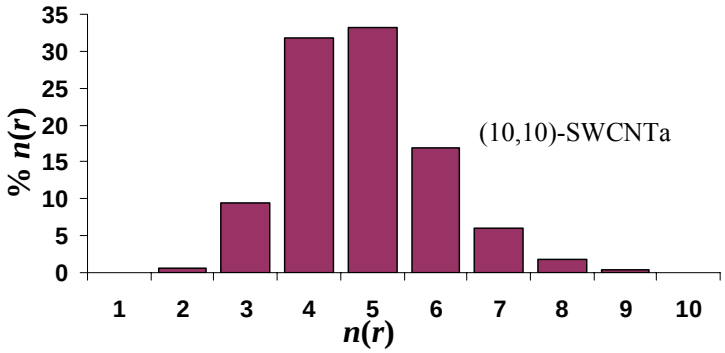

(b) water 102 molecules in (10,10)-SWCNTa

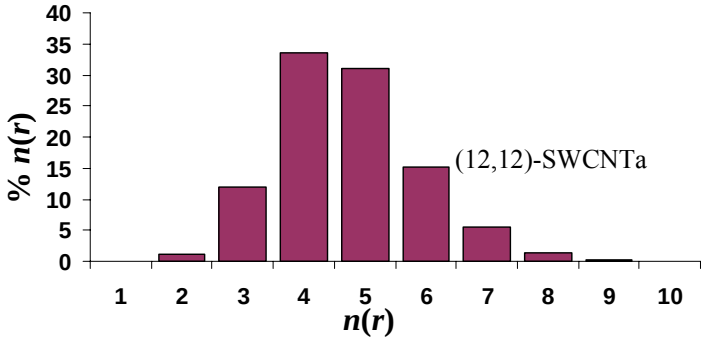

(c) water 162 molecules in (12,12)-SWCNTa

Figure A1 Histogram of coordination number distribution of water in SWCNTa ε_{co} = *0.114333* kcal mol^{-1}.

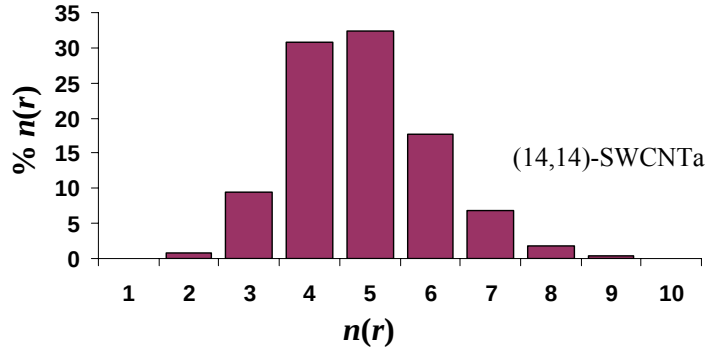

(d) water 237 molecules in (14,14)-SWCNTa

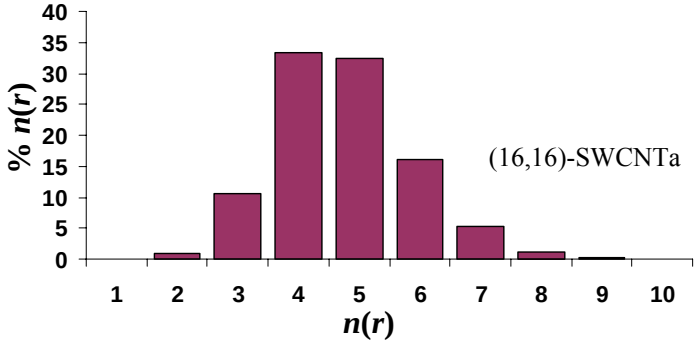

(e) water 327 molecules in (16,16)-SWCNTa

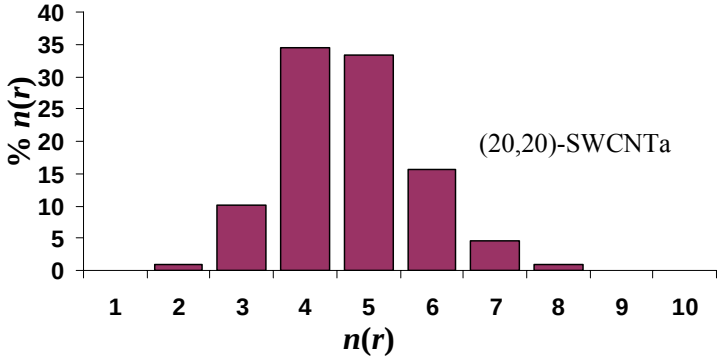

(f) water 547 molecules in (20,20)-SWCNTa

Figure A1 Histogram of coordination number distribution of water in SWCNTa ε_{co} = *0.114333 kcal* mol^{-1}. (cont'd)

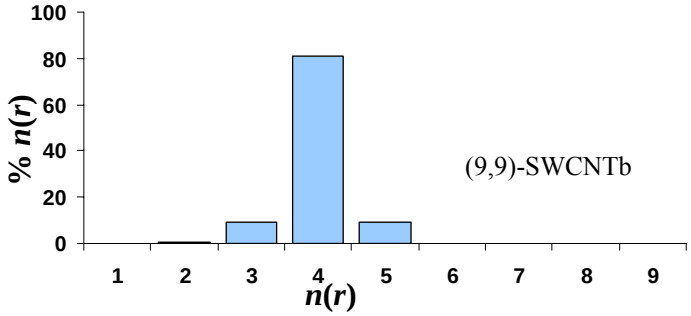

(a) water 77 molecules in (9,9)-SWCNTb

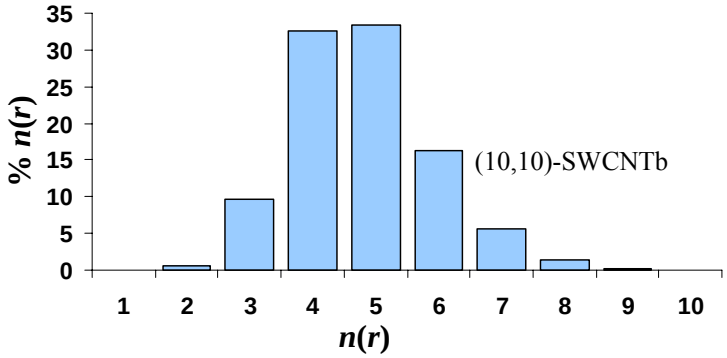

(b) water 102 molecules in (10,10)-SWCNTb

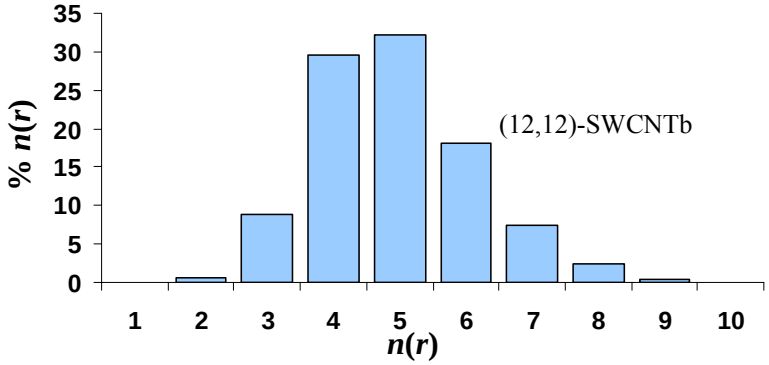

(c) water 162 molecules in (12,12)-SWCNTb

Figure A2 Histogram of coordination number distribution of water in SWCNTb ε_{co} = *0.12300* kcal mol^{-1} .

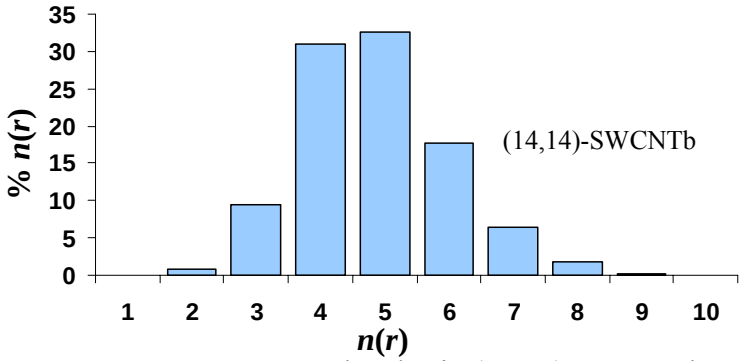

(d) water 237 molecules in (14,14)-SWCNTb

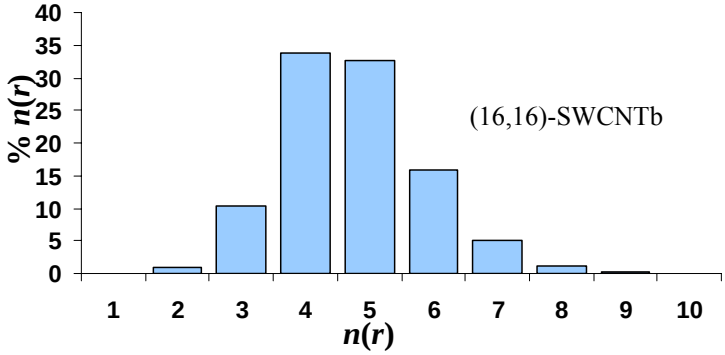

(e) water 327 molecules in (16,16)-SWCNTb

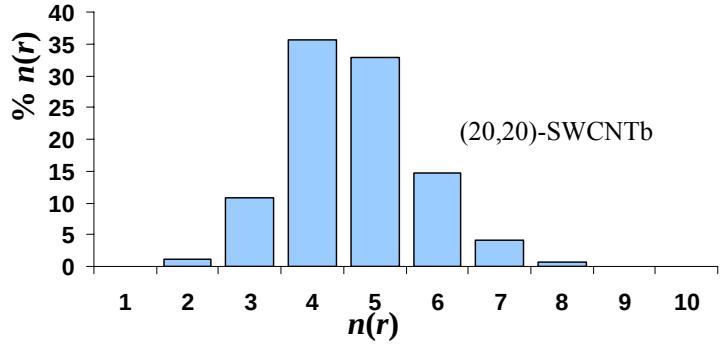

(f) water 547 molecules in (20,20)-SWCNTb

Figure A2 Histogram of coordination number distribution of water in SWCNTb ε_{co} = *0.12300* kcal mol^{-1} .

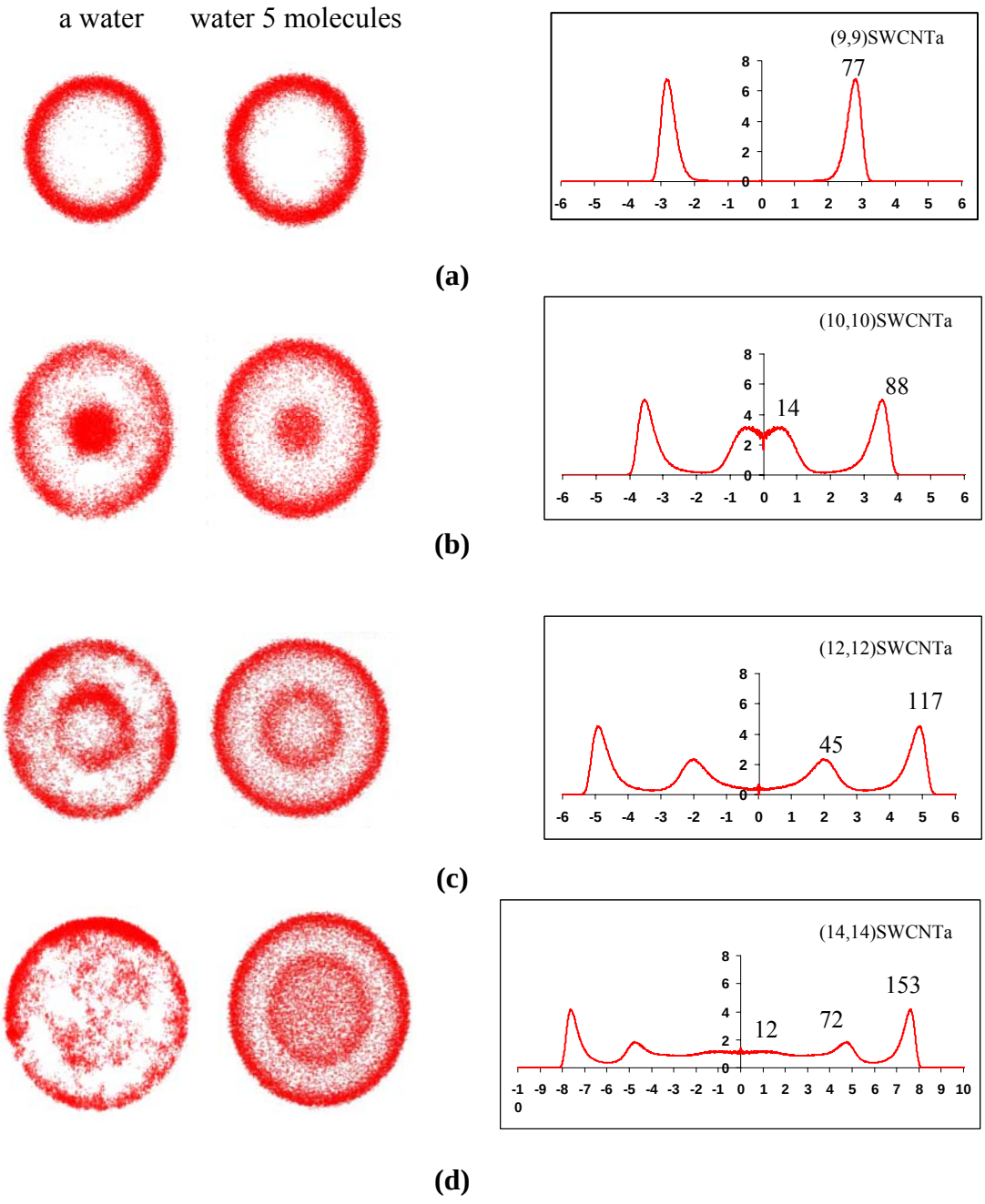

Figure A3 Cylindrical $g(r)$-function (*right*) of the water and trajectory plot of 1 (*left*) and 5 (*middle*) water molecules for the simulation of the (9,9)-**(a)**, (10,10)-**(b)**, (12,12)-**(c)**, (14,14)-**(d)**, (16,16)-**(e)** and (20,20)-**(f)** armchair SWCNTa (ε_{O-C} = *0.11433* kcal mol^{-1})

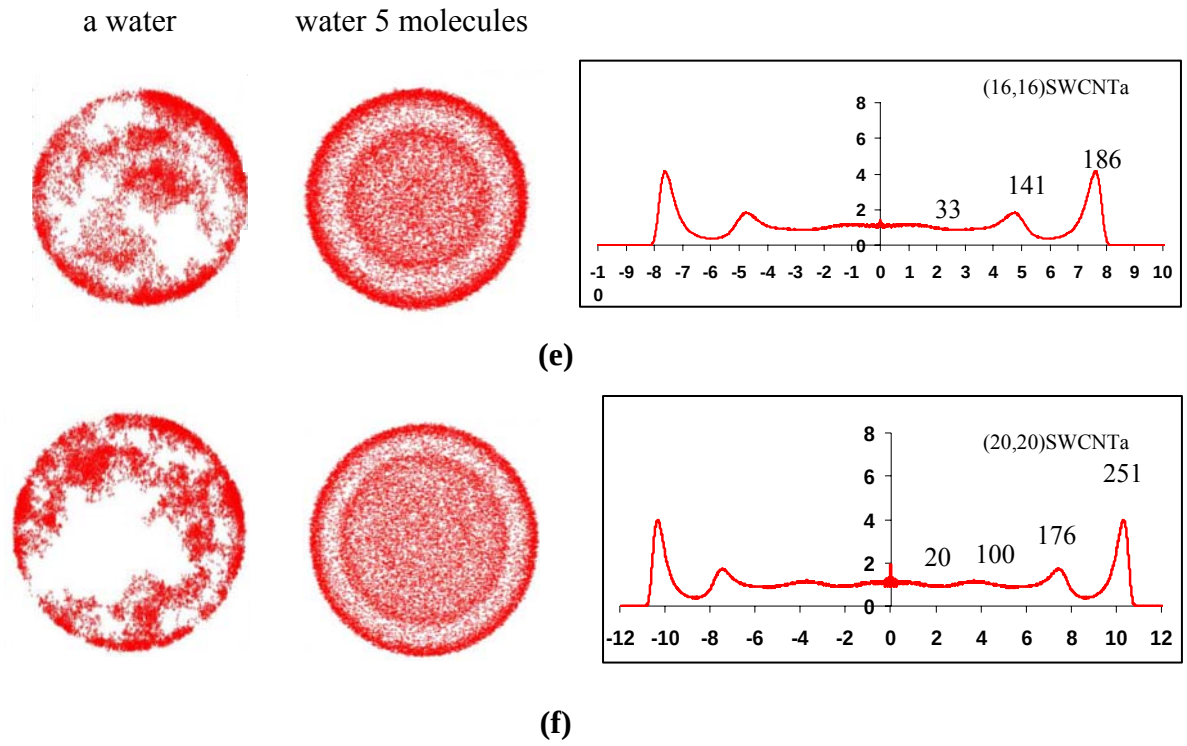

Figure A3 Cylindrical $g(r)$-function (*right*) of the water and trajectory plot of 1 (*left*) and 5 (*middle*) water molecules for the simulation of the (9,9)-**(a)**, (10,10)-**(b)**, (12,12)-**(c)**, (14,14)-**(d)**, (16,16)-**(e)** and (20,20)-**(f)** armchair SWCNTa (ε_{O-C} = *0.11433* kcal mol^{-1}). (cont'd)

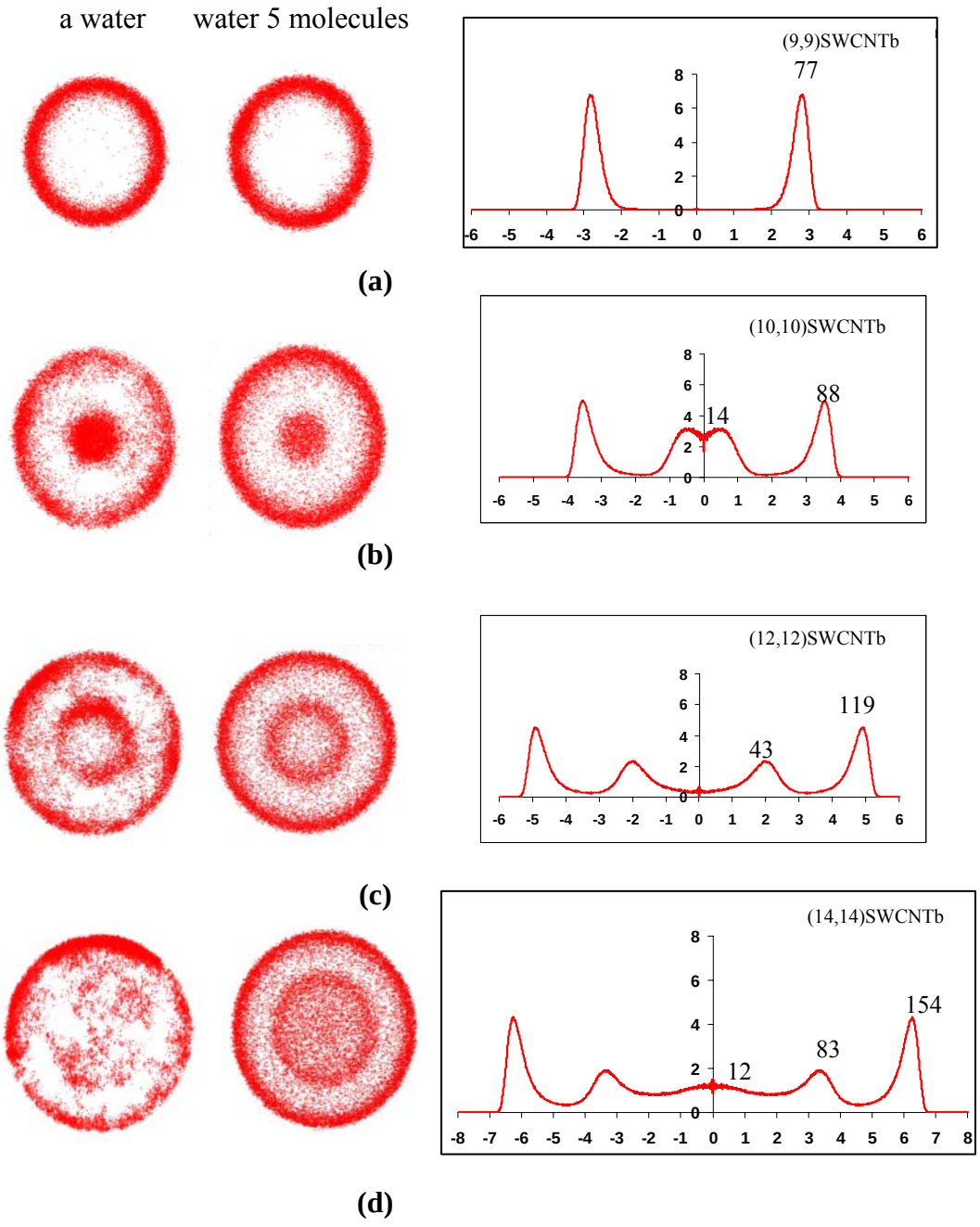

Figure A4 Cylindrical $g(r)$-function (*right*) of the water and trajectory plot of 1 (*left*) and 5 (*middle*) water molecules for the simulation of the (9,9)-**(a)**, (10,10)-**(b)**, (12,12)-**(c)**, (14,14)-**(d)**, (16,16)-**(e)** and (20,20)-**(f)** armchair SWCNTb (ε_{O-C} = *0.12300* kcal mol^{-1})

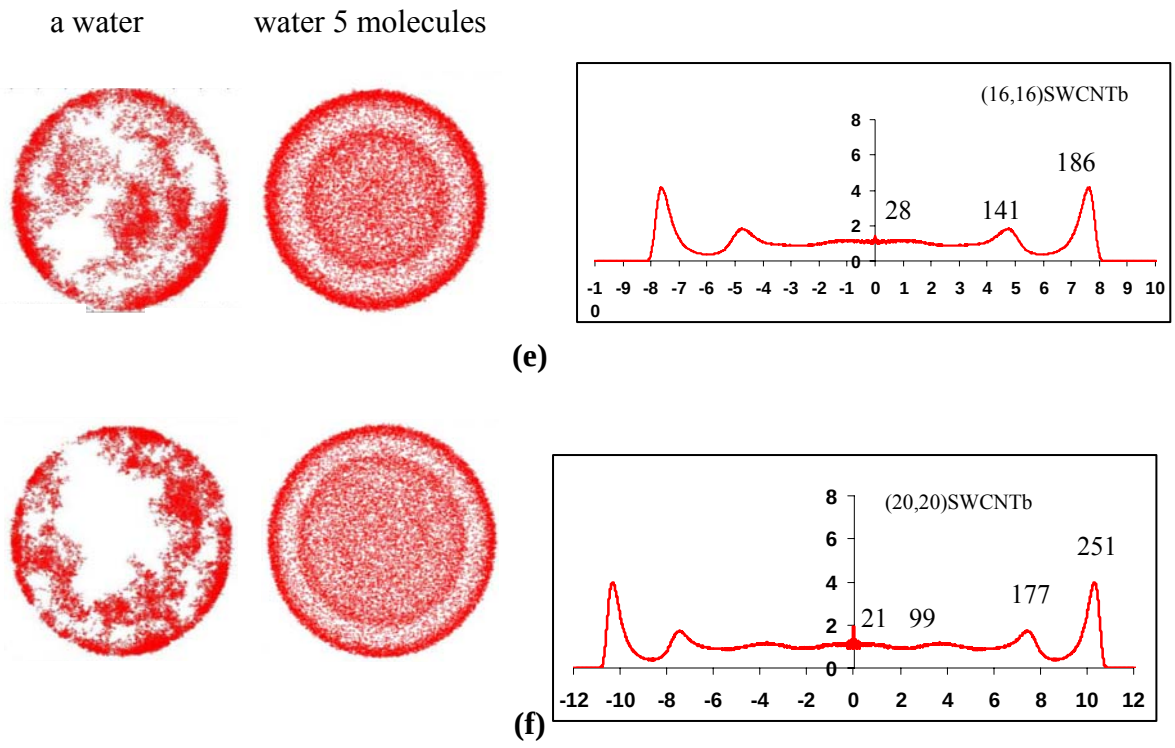

Figure A4 Cylindrical $g(r)$-function (*right*) of the water and trajectory plot of 1 (*left*) and 5 (*middle*) water molecules for the simulation of the (9,9)-**(a)**, (10,10)-**(b)**, (12,12)-**(c)**, (14,14)-**(d)**, (16,16)-**(e)** and (20,20)-**(f)** armchair SWCNTb ($\varepsilon_{O-C} = 0.12300$ kcal mol^{-1}).(cont'd)

Appendix B

Curriculum vitae and presentations

CURRICULUM VITAE

NAME : Miss Nongnuch Artrith

BIRTH PLACE : Maha Sarakham, Thailand

NATIONALITY : Thai

EDUCATION : 1997-2001, Khon Kaen University, B.Sc. (Physics)

SCHOLARSHIPS / AWARDS:

1. Thailand Research Fund (to JL)
2. Kasetsart University Research and Development Institute (KURDI)
3. National Nanotechnology Center (NANOTEC center of Excellence and Computational Nanoscience Consortium)
4. National Research Council of Thailand (NRCT)
5. Commission on Higher Education (Postgraduate Education and Research Programs in Petroleum, and Petrochemicals, and Advanced Materials and Postdoctoral Research Grants to TN), Ministry of Education
6. Graduate School Kasetsart University Fund
7. Research Assistant Scholarship, Kasetsart University
8. Innovative Leadership Award from National Science and Technology Development Agency (NSTDA), January 20-22, 2006.

(http://www.nstda.or.th/hrd/permanentcamp/activity/2006/leadercamp/index.html)

CONFERENCES / PRESENTATIONS:

a. **Molecular Dynamics Simulation Studies of Water Confined in SWCNTs and SWBNNTs.** (poster presentation)

Nongnuch Artrith, Tanin Nanok, Piboon Puntu and Jumras Limtrakul. Abstract of papers Congress on Pure and Applied Chemistry International Conference (PACCON 2008) January 30 - February 1, **2008**, 144.

b. **Structure and dynamics properties of water Confined in Nanotubes(CNTs and BNNTs) : A Molecular Dynamics Study**. (Oral presentation)

Nongnuch Artrith, Tanin Nanok, Piboon Puntu and Jumras Limtrakul. Proceeding of papers 33rd Congress on Science and Technology of Thailand (STT33), Walailak University, Thailand, October 18-20, **2007**, 199.

c. **The influence of -CH_3, -C_6H_5, -F, and –Carbon nanotubes on the hydrogen-bonded Adenine / Thymine adduct.** (Poster presentation)

Montree Sawangphruk, **Nongnuch Artrith,** Pipat Khongpracha and Jumras Limtrakul. Abstracts of Papers, 231st Congress on American Chemical Society National Meeting, Atlanta, GA, United States, March 26-30, **2006**, and oral presentation in 33rd Congress on Science and Technology of Thailand (STT31), Suranaree Universit of Technology, Thailand, October 18-20, **2005.**

Molecular Dynamics Simulation Studies of Water Confined in SWCNTs and SWBNNTs

Nongnuch Artrith[1, 2], Tanin Nanok[1, 2, 3], Piboon Pantu[1, 2, 3], Jumras Limtrakul [1, 2, 3]*

[1]*Laboratory for Computational and Applied Chemistry, Department of Chemistry, Faculty of Science, Kasetsart University, Bangkok 10900, Thailand*
[2]*Center of Nanotechnology, Kasetsart University Research and Development Institute, Kasetsart University, Bangkok 10900, Thailand*
[3]*NANOTEC Center of Excellence, National Nanotechnology Center, Kasetsart University, Bangkok 10900, Thailand*
**E-mail: jumras.l@ku.ac.th, Tel.662-562555 ext 2159, Fax 662-5625555 ext 2176*

Diffusion and molecular distribution of water confined in nanopores are important aspects for attaining scientific and technological features in the biological micro-fluidic systems. Here, we report the structure and dynamic properties of water confined in nanotubes using molecular dynamics (MD) simulations. The water density of 1.00 g/cm^3 was placed inside the periodic models of the (*n*,*n*)-armchair nanotubes (where *n* = 9, 12, 14, 16 and 20) for single-walled carbon nanotubes (SWCNTs) and boron nitride nanotubes (SWBNNTs) at the average temperature of 298 K. It was found that the confinement effect of narrow-pore nanotubes has a strong influence on both the molecular distribution and transport phenomena. Water molecules form the ice-like single-shell hexagonal structure inside the (9,9)-armchair SWCNT and SWBNNT, while multi-layered cylindrical structures are observed in larger nanotubes. In the largest studied nanotubes (20,20), water molecules can freely exchange between inner layers. The diffusion of water molecules through the (9,9)-SWBNNTs is twice faster than through the (9,9)-SWCNTs. This is due to the stronger van der Waals interaction between water and boron nitride nanotubes. The difference in diffusion rates between two types of nanotubes becomes small when the nanotube diameter increases.

REFERENCES

1. Tajkhorshid, E.; Nollert, P.; Jensen, M.; Miercke, L. J. W.; O'Connell, J.; Stroud, R. M.; Schulten, K. *Science*. **2002,** 296, 525-530.
2. Mashl, R. J.; Joseph, S.; Aluru, N. R.; Jakobsson, E. *Nano Lett*. **2003**, 3, 589-592.
3. Liu, Y.; Wang, Q.; Zhang L.; Wu, T. *J. Langmuir*. **2005**, 21, 12025-12030.
4. Liu, Y.; Wang, Q.; Wu. T., Zhang, L. *J. Chem. Phys*. **2005,** 123, 234701-234707.
5. Won, C. Y.; Aluru, N. R. *J. Am Chem. Soc*. **2007**, 129, 2748-2749.

ACKNOWLEDGEMENT

This work was supported in part by grants from the Thailand Research Fund (to JL) and the Kasetsart University Research and Development Institute (KURDI), the National Nanotechnology Center (NANOTEC center of Excellence and Computational Nanoscience Consortium), the National Research Council of Thailand (NRCT) and the Commission on Higher Education (Postgraduate Education and Research Programs in Petroleum, and Petrochemicals, and Advanced Materials and Postdoctoral Research Grants to TN), Ministry of Education. The support from the Graduate School Kasetsart University is also acknowledged.

การศึกษาสมบัติเชิงโครงสร้างและเชิงพลวัตของน้ำในท่อนาโนทิวบ์ โดยระเบียบวิธี Molecular Dynamics

STRUCTURE AND DYNAMIC PROPERTIES OF WATER CONFINED IN NANOTUBES: A MOLECULAR DYNAMICS STUDY

นงค์นุช อาจฤทธิ์[1,2], ธานิน นานอก[1,2], พิบูลย์ พันธุ[1,2], จำรัส ลิ้มตระกูล[1,2*]
Nongnuch Artrith[1,2], Tanin Nanok[1,2], Piboon Puntu[1,2], Jumras Limtrakul[1,2*]

[1] Physical Chemistry Division, Department of Chemistry, Faculty of Science, Kasetsart University, Bangkok 10900, Thailand
[2]Center of Nanotechnology, Kasetsart University Research and Development Institute, Bangkok 10900, Thailand
[*]Corresponding author: Tel. 662-294289000 ext 304, Fax 662-5625555 ext 2176, E-mail: jumras.l@ku.ac.th

บทคัดย่อ: การใช้ระเบียบวิธี Molecular Dynamics ศึกษาสมบัติเชิงโครงสร้างและเชิงพลวัตของน้ำที่ถูกจำกัดในท่อที่มีโครงสร้างระดับนาโนเมตร ณ อุณหภูมิห้อง พบว่าน้ำที่มีความหนาแน่น 1 กรัมต่อลูกบาศก์เซนติเมตร เมื่ออยู่ในท่อนาโนทิวบ์ชนิด คาร์บอน และ โบรอนไนไตรด์ ที่มีผนังชั้นเดียวแบบอาร์มแชร์ จะมีโครงสร้างการกระจายตัวและความเร็วในการเคลื่อนที่ตามแนวท่อแตกต่างกันไป ขึ้นอยู่กับขนาดเส้นผ่าศูนย์กลางของนาโนทิวบ์ โดยน้ำที่อยู่ในท่อนาโนทิวบ์ชนิด (9,9)-อาร์มแชร์ จะมีการจัดเรียงตัวคล้ายท่อน้ำแข็งรูปทรงกระบอกหกเหลี่ยมและมีผนังเพียงชั้นเดียว ต่างจากที่พบในท่อนาโนทิวบ์ขนาดใหญ่ขึ้นซึ่งมีการจัดเรียงตัวในลักษณะเป็นท่อหลายชั้นและระหว่างชั้นเกิดการแลกเปลี่ยนโมเลกุลของน้ำได้อย่างอิสระ อันเป็นสาเหตุสำคัญทำให้การแพร่ตามแนวท่อนาโนทิวบ์ขนาดใหญ่ช้ากว่าท่อขนาดเล็ก นอกจากนี้ยังพบว่าการแพร่ของน้ำในท่อนาโนทิวบ์ขนาดเล็กชนิด โบรอนไนไตรด์ มีอัตราเร็วกว่าในท่อนาโนทิวบ์ชนิด คาร์บอน เนื่องจากมีแรง adhesive force ภายในท่อสูงกว่า

Abstract: Structure and dynamic properties of water confined in nanotubes were investigated by using a molecular dynamics (MD) technique. The water density of 1.00 g/cm^3 was placed inside the periodic models of the single-walled armchair carbon nanotubes (SWCNTs) and boron nitride nanotubes (SWBNNTs) at the average temperature of 298 K. It was found that the confinement effect of narrow-pore nanotubes has a strong influence on both the molecular distribution and transport phenomena. The six-membered ring structure of the single-walled ice-like nanotube was observed in the (9,9)-armchair SWCNT and SWBNNT, while a multi-layered cylindrical structure was predicted in the large-pore nanotubes. In the latter cases, the water molecules can freely exchange between layers. This, consequently, causes a significant reduction of an axial diffusion coefficient. In narrow-pore systems, water molecules permeate through the BNNTs faster than through the SWCNTs. This is due to a stronger adhesive force generated from the attractive water-nanotube interactions in the BNNT systems.

Introduction: The transport phenomena and molecular distribution of water confined in nanopores have become important aspects for attaining scientific and technological features in the biological micro-fluidic systems and the delivery of beneficial molecules such as drugs, genes and biomolecules to the target cells [1,2]. Carbon nanotubes (CNTs) have gained much attention as prototypes for biological water channels due to their simplicity, stability, and nanoporosity. However, their electrical neutrality impedes them to reproduce some important features of biological channels, in terms of irregular surfaces and highly inhomogeneous charge distributions. Boron nitride nanotubes (BNNTs), an isoelectronic structure of CNTs, have been found to exhibit many superior properties and offer substantial advantages over CNTs such as a high Young's modulus, thermal conductivity and resistance to oxidation [3]. Furthermore, an alternating combination of boron and nitrogen atoms in their structure may mimic some characteristics of biological water channels better than CNTs. Therefore, the research on structural and dynamic properties of water confined in single-walled boron nitride nanotubes (SWBNNTs) is also of interest. Here, we report molecular dynamics simulations of water in different diameters of SWCNTs and SWBNNTs. The distribution and diffusion of water confined in nanotubes are discussed.

Methodology: The molecular dynamics simulations were performed in the *NVT* ensemble at the average temperature of 298 K using a time step of 1 fs. Coordinates and velocities of atoms were stored every 50 fs of 1 ns after the equilibration period of 0.3 ns for the subsequent analysis. The self-diffusion coefficients were determined by using the Einstein relation. All simulations were executed by using the DL_POLY 2.0 program. The systems studied were periodic rigid models of the (*n*,*n*)-armchair SWCNTs and SWBNNTs of a fixed length of 36.89 Å. The (*n*,*n*)-armchair nanotubes were in series *n* = 9, 12, 14, 16, and 20 which correspond to the effective diameters of 8.86, 12.92, 15.62, 18.34 and 23.74 Å, respectively. These nanotubes were filled with a certain number of water molecules at a density of 1.0 g/cm^3. Water was described with the extended simple point charge (SPC/E) model [4], while the water-nanotube interactions were described by only a short-range Lennard-Jones potential with $\varepsilon =$ 0.1230, 0.1216, and 0.1502 kcal/mol for C-O, B-O, and N-O interactions, respectively, and $\sigma_{C\text{-}O} = \sigma_{B\text{-}O} = \sigma_{N\text{-}O} = 3.26$ Å.

Table 1. Axial self-diffusion coefficients ***D*** (cm^2/s) of water in SWCNTs and SWBNNTs at the average temperature of 298 K and the water density of 1.00 g/cm^3.

Model	***D*** (cm^2/s)	Model	***D*** (cm^2/s)
(9,9)-armchair SWCNT	67.88 x 10^{-5}	(9,9)-armchair SWBNNT	152.85 x 10^{-5}
(12,12)-armchair SWCNT	15.02 x 10^{-5}	(12,12)-armchair SWBNNT	21.79 x 10^{-5}
(14,14)-armchair SWCNT	7.65 x 10^{-5}	(14,14)-armchair SWBNNT	8.27 x 10^{-5}
(16,16)-armchair SWCNT	3.53 x 10^{-5}	(16,16)-armchair SWBNNT	4.23 x 10^{-5}
(20,20)-armchair SWCNT	1.68 x 10^{-5}	(20,20)-armchair SWBNNT	4.09 x 10^{-5}

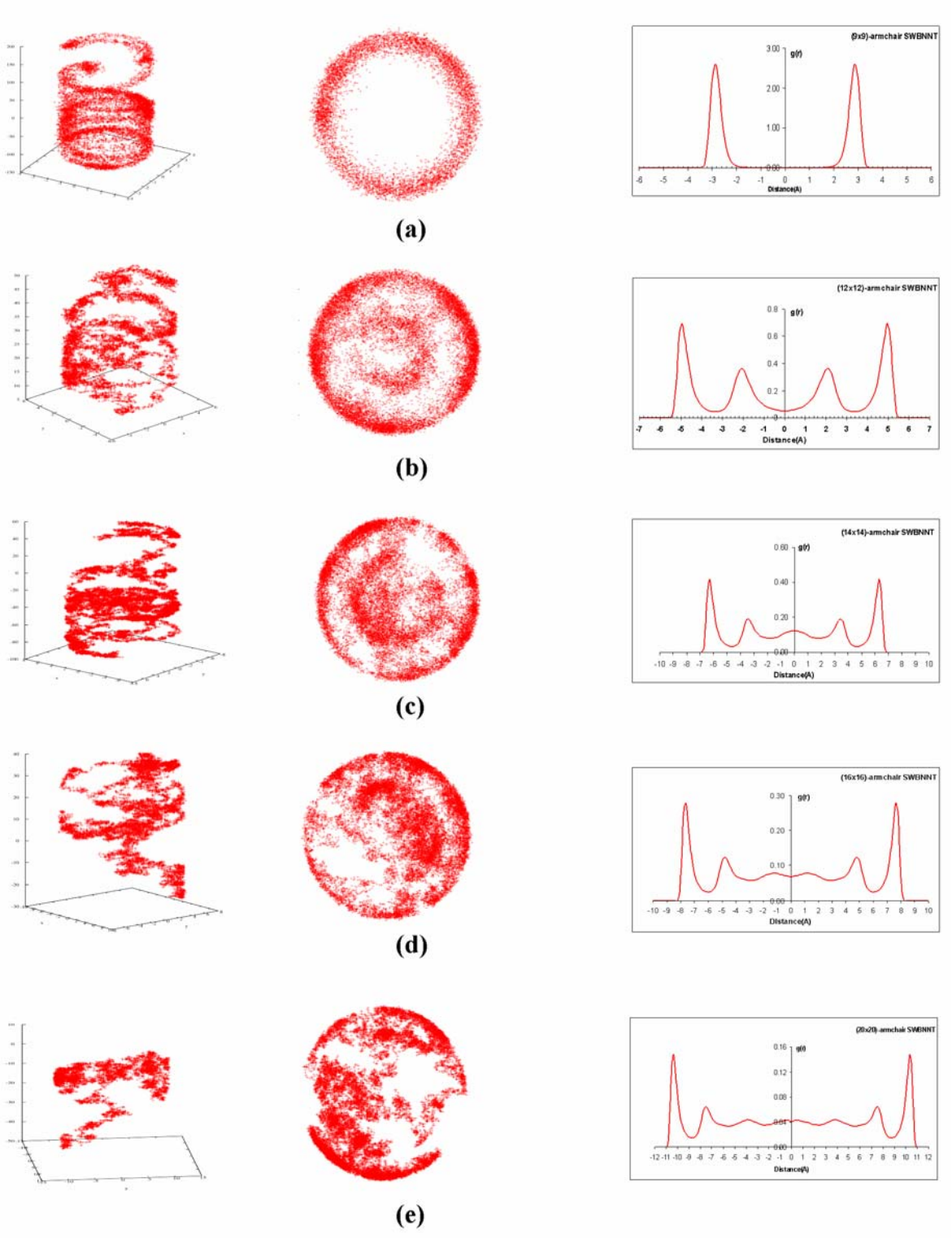

Figure 1. Three-dimensional trajectories (left) of a selected water molecule in (9,9)- (a), (12,12)- (b), (14,14)- (c), (16,16)- (d) and (20,20)- (e) armchair SWBNNTs; their

projections onto the *xy* plane (middle); and cylindrical $g(r)$ distribution functions of water with respect to the center of those SWBNNTs (right).

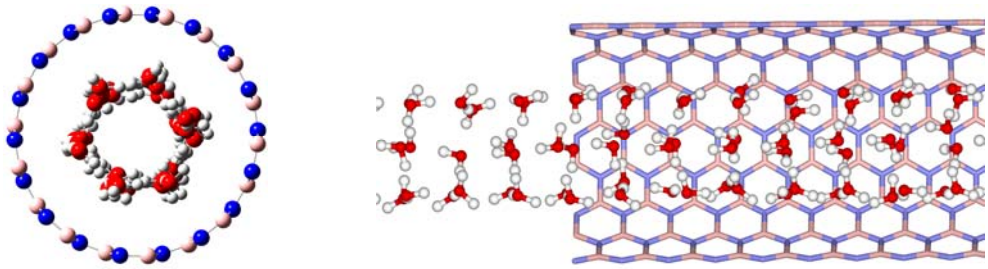

(a) **(b)**

Figure 2. Top view (a) and side view (b) of a snap short of the six-membered ring structure of the single-walled ice-like nanotube in a (9,9)-armchair SWBNNTs.

Results, Discussion and Conclusion: Dynamic properties of water confined in various nanotubes were expressed in terms of its self-diffusion coefficient along the nanotube axis. The self-diffusion coefficients of water in different diameters of both SWCNTs and SWBNNTs are listed in Table 1. In both types of nanotube, the calculated self-diffusion coefficient decreases as the nanotube diameter increases. This occurrence can be explained by tracing the molecular trajectory of water molecules throughout the simulation run. In the (9,9)-armchair nanotubes, the smallest diameter nanotube studied, the track picture of their trajectory resembles a circular helix (Figure 1a). Over this timescale, the motion of one water molecule is highly correlated with that of the neighbouring water molecules. As a result, they move together in the same direction along the nanotube length. Furthermore, the water in this narrow pore was conducted to form the six-membered ring structure of single-walled ice-like nanotube (Figure 2). The exchange of water molecules between adjacent positions is intractable, and thus the axial diffusion becomes forceful. In the larger diameter nanotubes, the multi-layered water nanotube is observed (Figures 1b-e). The resulting cylindrical $g(r)$ distribution functions (Figures 1b-e) of water with respect to the centre of the nanotubes show the non-zero minimum values of the function between neighbouring peaks, indicating that the exchange of water molecules between layers becomes possible. This results in the reduction of an axial self-diffusion coefficient in the large-pore nanotubes. Comparing between the same pore sizes of SWCNTs and SWBNNTs, it was found that the axial diffusion of water in the SWBNNTs is faster than that in the SWCNTs. This may be understood in terms of the adhesive force generated from the attractive interactions between water and nanotubes.

References:

(1) Liu, Y., Wang, Q., Zhang L., Wu, T. *J. Langmuir*. 2005. **21**, 12025-12030.
(2) Liu, Y., Wang, Q., Wu. T., Zhang L. *J. Chem. Phys*. 2005 **123**, 234701-234707.
(3) Won, C, Y., Aluru, N, R. *J. Am Chem. Soc*. 2007, **129**, 2748-2749.

(4) Lyubartsev, A. P., Laaksonen, A. *J. Phys. Chem.* 1996**, 100***,* 16410-16418.

Keywords: Water, Molecular dynamics (MD), Carbon nanotubes (CNTs), Boron Nitride nanotubes (BNNTs).

Acknowledgements: We gratefully acknowledge the Commission of Higher Education (CHE), the Graduate School Kasetsart University funds, Thailand Research Fund (TRF Senior Research Scholar to JL) and NANOTEC Center of Excellence at Kasetsart University for funding this research.

การศึกษาทางทฤษฎีของอิทธิพลของหมู่ เมทิล ฟีนิล ฟลูโอไรด์ และ ท่อคาร์บอนนาโน ที่แทนที่บนอะดีนีนต่อพันธะไฮโดรเจนของ คู่เบส อะดีนีน และไทมีน ในดีเอนเอ

THE INFLUENCE OF -CH_3, -C_6H_5, -F, AND –CNT ON THE HYDROGEN-BONDED ADENINE/THYMINE ADDUCT

มนตรี สว่างพฤกษ์[1,2], นงค์นุช อาจฤทธิ์[1,2], พิพัฒน์ คงประชา[1,2], จำรัส ลิ้มตระกูล[1,2,*]

Montree Sawangphruk[1,2], Nongnuch Artrith[1,2], Pipat Khongpracha[1,2], Jumras Limtrakul[1,2]
[1] Laboratory for Computational & Applied Chemistry, Department of Chemistry, Faculty of Science, Kasetsart University, Bangkok 10900, Thailand
[2] Center of Nanotechnology, Kasetsart University, Bangkok 10900, Thailand;
e-mail address: fscijrl@ku.ac.th (J. Limtrakul)

บทคัดย่อ: ศึกษาสมบัติเชิงโครงสร้างและพลังงานของคู่เบส อะดีนีน และไทมีน ในดีเอนเอ ที่ถูกแทนที่ด้วยหมู่ เมทิล ฟีนิล ฟลูโอไรด์ และท่อ คาร์บอนนาโน ด้วยระเบียบวิธีการคำนวณแบบ ONIOM(6-31G(d,p):AM1) พบว่าอิทธิพลของหมู่เมทิล ฟีนิล และ ท่อคาร์บอนนาโน มีผลต่อพลังงานและความยาวพันธะไฮโดรเจนของคู่เบส อะดีนีน และไทมีนในดีเอนเอน้อยกว่าอิทธิพลของหมู่ฟลูโอไรด์ ทั้งนี้เนื่องจากหมู่ เมทิล ฟีนิล และ ท่อคาร์บอนนาโน คือหมู่ที่ให้อิเล็กตรอนแก่โมเลกุลของอะดีนีนในขณะที่หมู่ฟลูโอไรด์เป็นหมู่ดึงอิเล็กตรอนจากโมเลกุลของอะดีนีน ส่วนอิทธิพลของการแทนที่ด้วยท่อคาร์บอนนาโน ตรงตำแหน่งด้านข้างและด้านปลายของท่อคาร์บอนนาโน พบว่าการแทนที่ที่ปลายท่อ ส่งผลให้พันธะไฮโดรเจนของคู่เบสมีความเสถียรมากขึ้นกว่าการแทนที่ตรงตำแหน่งด้านข้างนอกจากนั้นจากการวิเคราะห์การเปลี่ยนแปลงของประจุของอะตอมภายในโมเลกุลยังให้ผลสอดคล้องกับการเปลี่ยนแปลงทางโครงสร้างและพลังงาน

Abstract: The geometries and energies of base pairs of T:A-COR are calculated at B3LYP/6-31G(d,p) level for R=CH_3, C_6H_5 and F and at ONIOM(B3LYP/6-31G(d,p):AM1) level for R= Carbon Nanotubes. Frontier molecular orbital (FMO) analysis and natural bond orbital (NBO) analysis have been carried out on the optimized geometries. The charge distribution and bonding analysis have also been investigated. The results show that the stabilization energy decreases when the –COR groups are substituted at the reactive amino group of adenine via peptide bond. The NBO analysis shows the charge transfer between the two monomers of the A:T base pair derivatives. The decrease in the hydrogen bond strength is correlated with the substituting groups.

Introduction: Since Iijima discovered carbon nanotubes (CNTs) in 1991, these materials have fascinated a myriad of investigators for their distinct structural, electrical, mechanical, and electromechanical properties. The use of nanotubes in biological applications is one of the most important applications, such as artificial muscles (actuators), nanotube field-effect transistors, nanotube-DNA electrochemical sensors and biomedical sensors. The concept of using DNA to direct the assembly of nanotubes into nanoscale devices is also attracting attention because of its potential to assemble a multicomponent system in one step by using different base sequences for each component. So far, the focus in this area has been on placing DNA at the tips and the side walls of nanotubes. To produce reactive sites to which the DNA may be attached, the nanotubes are mainly oxidized by nitric acid (HNO_3) treatment to introduce carboxyl groups on their tips; this procedure also introduces carboxyl groups at the sidewalls. DNA molecules with functional linkers are then coupled to the carboxyl groups on the nanotubes. In this work, to know the effect of CNTs to the hydrogen bonds on the A:T base pair of DNA, peptide bond is constructed by using the acid-base reaction between adenine and a carboxylic group of carbon nanotubes. This reaction is focused only on the reactive site of adenine that is the secondary amino (NH9) of adenine,

like the reaction between adenine and deoxyribose in the DNA formation. To understand the effect of the substuents to the hydrogen bonds on the A:T base pair, we have constructed the model, T:ACOR where R are CH_3, C_6H_5, F, tip-CNT and side-CNT.

Methodology: The geometries and energies of base pairs of T:A-COR are calculated by using the GAUSSIAN 03 program at B3LYP/6-31G(d,p) level for R = CH_3, C_6H_5 and F and at the ONIOM(B3LYP/6-31G(d,p):AM1) level for R = carbon nanotubes. The counter poise correction method was used to correct the basis set superposition error (BSSE) for all binding energies portrayed in this work. The T:ACO-nanotubes were taken and are represented in Figure 1, in which the high-level part contains 16 carbon atoms (see the ball and stick atoms in Figure 1). Such an ONIOM (B3LYP/6-31G (d,p):AM1) approach and a modeling scheme were utilized in our previous study of the Diels Alder cycloadditions of single-wall carbon nanotubes with electron-rich dienes. A similar ONIOM model was used in other groups in the theoretical studies of carbon nanotubes, such as the base-catalyzed [2,3] cycloaddition of transition metal oxide (OsO_4) on [5,5] SWNT and the 1,3-dipolar cycloaddition onto the sidewalls of [5,5] SWNT. At the same time, frontier molecular orbital (FMO) analysis and natural bond orbital (NBO) analysis have been carried out on the optimized geometries. The charge distribution and bonding analysis have also been investigated.

Results, Discussion and Conclusion: It was found that two calculated hydrogen bond lengths in A:T are 2.94 and 2.84 Å, which approach to 2.95 and 2.82 Å of X-ray. On the other hand, the BSSE-corrected energy of A:T is -12.35 kcal/mol, which is in reasonable agreement with -12.10 kcal/mol of the experimental value. These suggest that the results of DFT calculation at B3LYP/6-31G(d,p) level is comparable with the experimental X-ray crystallography data. In case of ($COCH_3$)-A:T and (COC_6H_5)-A:T, both methyl and benzyl groups are the slight electron donating groups, which lead to the similar result of -12.70 kcal/mol of relative energies. The (COF)-A:T is, in contrast, more exothermic than ($COCH_3$)-A:T and (COC_6H_5)-A:T because the fluoride group is the strong electron withdrawing group. For (9-carbonyl tip-[5, 5]-SWNT)-A:T and (9-carbonyl sidewall-[5, 5]-SWNT)-A:T, we found that the former complex gives -12.34 kcal/mol of corrected energy and the latter complex provides -11.64 kcal/mol of corrected energy. This is due to the effect of electron delocalize existing only in case of (9-carbonyl tip-[5, 5]-SWNT)-A. FMO and NBO analyses have, in addition, confirmed the alteration of structures and energies (see Figure 1 and Table 1).

Table 1 Bond lengths (pm) of base pairs optimized at ONIOM(B3LYP/6-1G(d,p):AM1).

Models	Bond lengths (pm)					
	O4'-N6	O4'-H6	N6-H6	N1-N3'	N1-H3'	N3'-H3'
A:T	294.0**(1)**	192.1**(1)**	102.2**(5)**	284.5**(6)**	179.7**(6)**	104.9**(1)**
($COCH_3$)-A:T	293.0**(4)**	191.0**(4)**	102.3**(2)**	285.7**(3)**	181.1**(3)**	104.6**(4)**
(COC_6H_5)-A:T	293.3**(3)**	191.3**(3)**	102.3**(2)**	285.3**(5)**	180.6**(5)**	104.7**(2)**
(COF)-A:T	291.9**(6)**	189.8**(6)**	102.4**(1)**	286.6**(1)**	182.2**(1)**	104.4**(6)**
(CO-side-SWNT)-A:T	293.5**(2)**	191.6**(2)**	102.2**(5)**	285.6**(4)**	181.0**(4)**	104.7**(2)**
(CO-tip-SWNT)-A:T	292.8**(5)**	190.7**(5)**	102.3**(2)**	285.9**(2)**	181.4**(2)**	104.6**(4)**

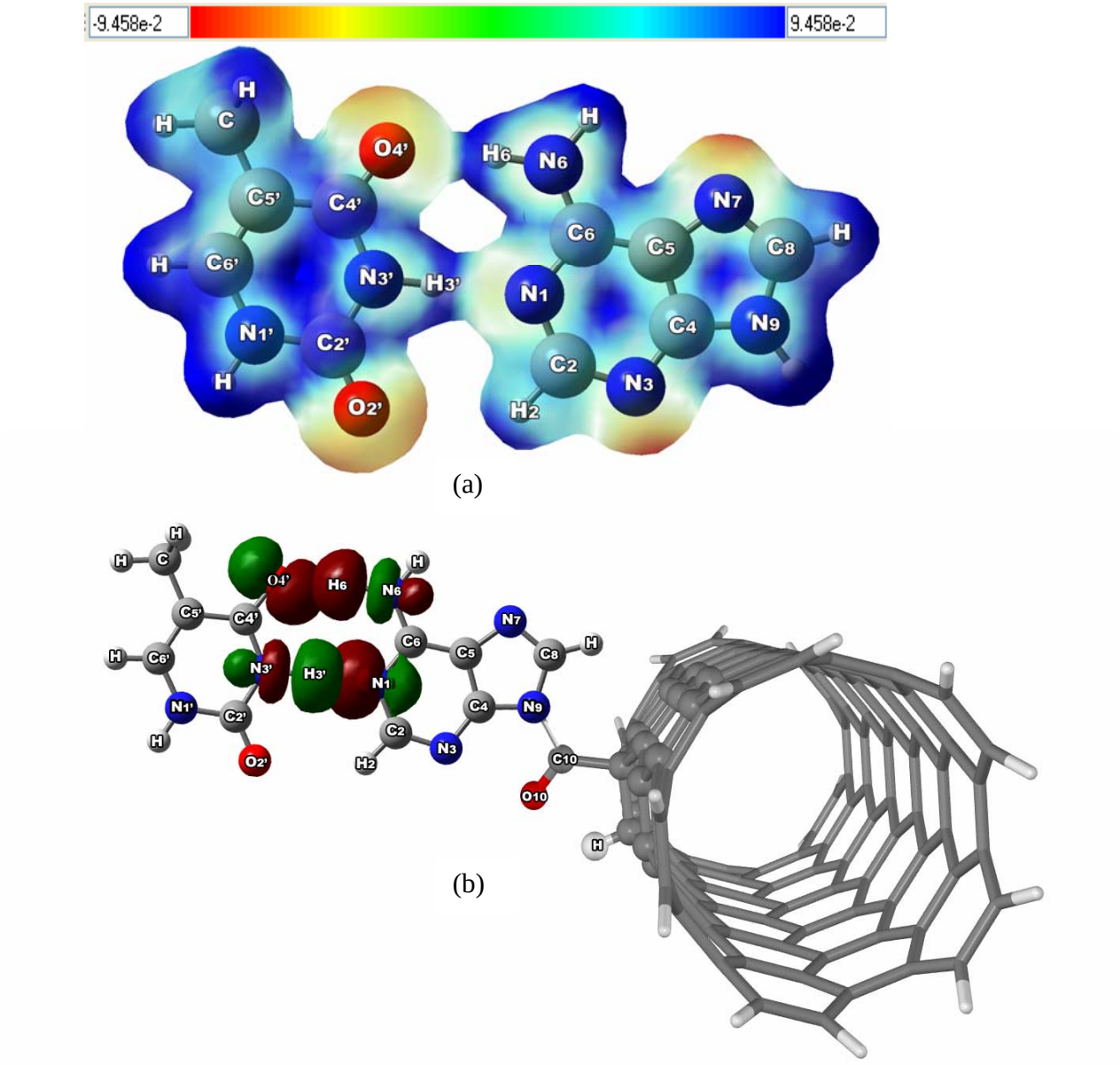

Figure 1 (a) The electrostatic potential is mapped onto a particular value of the total SCF electron density of A:T base pair.

(b) Orbital interaction of (RCO)-A:T where R is a sidewall SWNT.

References:

(1) Sumio Iijima (1991) *Nature*, **354**, 56-58.
(2) Richard E. Smalley (1998) *Nature*, **391**, 59-62.
(3) Supawadee Namuangruk, Piboon Pantu and Jumras Limtrakul (2004) *Journal of Catalysis*, **225**, 523-530.
(4) Supawadee Namuangruk, Piboon Pantu and Jumras Limtrakul (2005) *Journal of Chemical Physics and Physical Chemistry*, **6**, 1333-1339.
(5) Chompunuch Warakulwit, Suwassa Bumrungsap, Pataraporn Luksirikul, Pipat Khongpracha and Jumras Limtrakul (2005) *Studies in Surface Science and Catalysis*, **156**, 823-828.

Keywords: Carbon nanotubes, Base pairs, A:T.